Dmitrijs Guzs

COST EFFECTIVE INNOVATIVE SOLUTION FOR TRANSMISSION CAPACITY MANAGEMENT IN LOW-INERTIA WEAKLY INTERCONNECTED POWER SYSTEMS

Doctoral Thesis

RIGA TECHNICAL UNIVERSITY

Faculty of Electrical and Environmental Engineering
Institute of Power Engineering

Dmitrijs Guzs

Doctoral Student of the Study Program "Power and Electrical Engineering"

Cost effective, innovative solution for transmission capacity management in low-inertia weakly interconnected power systems

Doctoral Thesis

Scientific supervisors
Professor *Dr. habil. sc. ing.*
ANTANS SAUHATS
Assoc. Professor *Dr. sc. ing.*
ANDREJS UTANS
Assoc. Professor *PhD*
GATIS JUNGHANS

Riga 2023

ABSTRACT

The topic of climate change and the actions to combat it on a global scale have led to several fundamental developments in the global energy systems and particularly – in the power systems. These developments include decommissioning of conventional fossil fueled power plants and a massive introduction of renewable non-synchronous power plants, leading to massive reductions of system inertia in the power systems.

The political decisions for desynchronizing the Baltic power system from UPS/IPS power grid and synchronizing it to the ENTSO-E grid are firm. This development will lead to Baltic power system becoming a weakly interconnected system, working in island mode occasionally and with rapidly diminishing system inertia levels due to the plans for massive introduction of renewable power plants.

A novel, predictive, rapid load shedding (LS) method/scheme is proposed to tackle the challenges stated above. The proposed novel LS scheme is based on using synchronous condensers as frequency/ROCOF sensors and triggering the LS much quicker than a conventional LS would do. In such wise, power system frequency can be stabilized in the case of a major loss-of-generation contingency and be held within the safe frequency threshold avoiding a potential system blackout.

The proposed novel LS scheme has been tested on the case of Baltic power system in island mode and showed significant positive effect of the system frequency stability. The results show that, with the scheme implemented, the frequency fall during contingencies is significantly reduced when comparing to the conventional LS and the positive effect on the system frequency strongly correlates with the diminishing system inertia levels.

The effect of the novel LS scheme on the socio-economic welfare (SEW) of the power system has been tested on the case of Baltic power system for both historic (year 2020) and future (years, 2030, 2040, 2050) cases. The results show that implementation of the scheme could bring multi-million EUR benefits to Baltic power grid users annually and these benefits of the scheme are vastly superior over both expected load shedding costs and over the capital expenses for implementing the proposed LS scheme.

Showing both system-related and fiscal effects the proposed LS scheme positive, the implementation of proposed LS scheme may become an important part of the Baltic power system transformation into a CO_2-neutral, stable and independent power grid.

ANOTĀCIJA

Klimata izmaiņas temats un globālā mēroga darbības šo izmaiņu apkarošanai ir veduši uz vairākām fundamentālām attīstības tendencēm globalajās enerģētiskās sistēmās un it īpaši – elektriskajās energosistēmās. Šīs tendences iekļauj sevī konvencionālo fosilo elektrospēkstaciju ekspluatācijas pārtraukšanu un atjaunojamo asinhrono enerģijas avotu masīvo ekspluatācijā ieviešanu, novedot pie elektrisko energosistēmu inerces līmeņu masīvo samazināšanos.

Ir pieņemti politiskie lēmumi Baltijas energosistēmas atslēgšanai no Krievijas apvienotā energotīkla un sinhronizācijai pie ENTSO-E energotīkla. Šī darbība novedīs pie ta, ka Baltijas energosistēma kļūs vāji savienota, ar riskiem salas režīma darbībai un ar ātri sarūkošo inerces līmeni atjaunojamo energoresursu masīvo ekspluatācijā ieviešanas dēļ.

Lai tikt galā ar augstāk norādītiem izaicinājumiem, tiek ierosināts ieviest jaunu, prediktīvo, ātro atslodzes automātikas metodi/shēmu. Piedāvātā atslodzes automātikas shēma ir balstīta uz sinhrono kompensatoru kā frekvences/ROCOF sensoru izmantošanas, un šīs shēmas aktivizācija notiek daudz ātrāk salīdzonot ar esošo frekvences atslodzes automātiku. Šādā veidā energosistēmas frekvence var tikt stabilizēta lielo frekvences avāriju (lielo ģenerējošo iekārtu atslēgumu) gadījumā un tādējādi frekvence var tikt noturēta drošās robežas, izvairoties no potenciālā sistēmas blekauta/nodzēšanas.

Piedāvātā atslodzes shēma ir tikusi pārbaudīta simulējot uz Baltijas energosistēmas salas režīma gadījuma, un simulācijas parādīja ievērojamu pozitīvu ietekmi uz energosistēmas frekvences stabilitāti. Rezultāti ir parādījuši, ka piedāvātā shēma spēj būtiski ierobežot energosistēmas frekvences kritumu frekvences avāriju gadījumos salīdzinot ar esošo frekvences atslodzes automātiku. Šis pozitīvais efekts uz frekvencei stirpi korelē ar energosistēmas inerces līmeņa samazinājumu.

Piedāvātā atslodzes shēma ir tikusi pārbaudīta uz pienesumu Baltijas energosistēmas socioekonomiskai labklājībai, simulācijām izmantojot gan vēsturiskus ieejas datu (2020. g.), gan prognozētus ieejas datus (2030., 2040, 2050. g.). Rezultāti ir parādījuši, ka piedāvātās shēmas ieviešana varētu ietaupīt Baltijas energosistēmas lietotājiem vairākus miljonu EUR gadā, un šie piedāvātās shēmas pienesumi ir daudzkārt lielāki pār sagaidāmām patērētāju atslēgumu izmaksām un kapitālizmaksām piedāvātās atslodzes shēmas praktiskai ieviešanai energotīklā.

Parādot gan pienesumus energosistēmas frekvences stabilitātei, gan pienesumus socioekonomiskai labklājībai, piedāvātā atslodzes automātikas shēma varētu kļūt par Baltijas energosistēmas transformācijas CO_2-neitrālā, stabilā un neatkarīgā tīklā neatņemamu sastāvdaļu.

CONTENTS

ABBREVIATIONS

AC – alternating current
AST – AS Augstsprieguma Tīkls
BPP – biomass power plant
BPS – Baltic Power System
CE – continental Europe
CHP – combined heat and power plant
CI – congestion income
DC – direct current
ENS – energy not served
ENTSO-E - European Network of Transmission System Operators
EPS – energy power system
EU – European Union
EV – electric vehicle
FCR – frequency containment reserve
FR – frequency relay
FRR – frequency restoration reserve
mFRR – manual frequency restoration reserve
HPP – hydro power plant
sHPP – small hydro power plant
HV – high-voltage
HVDC – high-voltage direct current
IED - intelligent electronic device
LS – load shedding
LSC – load shedding costs
MEPP – most expensive power plant
MV – medium-voltage
NEMO – nominated electricity market operator
PMU – phase measurement unit
PSHPP – pumped-storage hydro power plant
RES – renewable energy sources
ROCOF – rate of change of frequency
RR – replacement reserve
RTU – Riga Technical University
SC – synchronous condenser
SDAC – single day-ahead coupling (of European power markets)
SEW – socio-economic welfare
SF – Simulation Facility
SOGL – System Operation Guideline
SPP – solar power plant
SSR – security, stability, resilience

TSO – transmission system operator
UFLS – under-frequency load shedding
UMM – urgent market message
UPS/IPS – unified/independent power system of Russia
VOLL – value of lost load
WPP – wind power plant

LIST OF FIGURES

LIST OF TABLES

INTRODUCTION

Topicality of the research

With the importance of the problem of climate change being widely recognized by the global community [1] and with the need to solve this problem by reducing the carbon emissions, the energy systems of the developed countries are currently going through a major transformation. The executive goal of the forthcoming transformation is to reach net zero carbon emissions by 2050 in order to hold the 1.5°C climate target and is called the "energy transition" [2]. This includes transformation of all energy-intensive sectors of the economies: power generation, transmission and distribution, supply and consumption of heat and fuel, transport, agriculture, households etc. and is done by replacing fossil energy sources with carbon-neutral/renewable ones as well as by electrification. Despite the fact that the goal is unambiguously defined and the way to achieve it is transparent, it is already clear that a number of serious problems and obstacles will arise, caused by:

• massive shutdown of the existing conventional electric power generation capacity including nuclear and the urgent need to replace this capacity [2].

• tripling of the level of electric power generation of electricity by 2050 compared to today's level with renewables providing for 90% of the total volume [2].

• intermittency of the renewable energy sources mainly driven by the weather conditions; in some regions this intermittency is additionally amplified by the reliance on cogeneration power plants driven solely by the heat demand.

• power generation structure tending from centralized to decentralized/scattered generation.

• the planned carbon net zero energy system is still supposed to stay sustainable, secure, affordable and resilient [3].

The penetration of the power systems with intermittent renewable energy sources brings a major paradigm change for the field of electric power supply. Not only are these generation sources uncontrollable, but they are also non-synchronous – that is they produce power without involvement of rotating electrical synchronous machines as synchronous generators.

The mentioned factors are partially self-contradicting, so the necessity to simultaneously achieve all of these leads to a complex problem which can only be solved through global and inter-disciplinary cooperation with the participation of technology developers and manufacturers, generating companies, transmission and distribution network operators and millions of consumers. The problem is exacerbated by the growing interconnection between various engineering infrastructures. The power supply process can be disrupted by the occurrence of malfunctions in communication systems, water supply, transport, etc. Gas supply can disrupt power supply and vice versa. On the other hand, even short-term power outages can cause huge economic losses and tragic consequences arising from the paralysis of life in cities and countries. Extremely large losses occur in cases of large-scale blackouts in power systems. Most of the large-scale blackouts observed in power systems are triggered by random events

which lead to loss of power system stability. Therefore, it is of principal importance to maintain the stability and uninterruptibility of the power supply during the energy transition [3].

Energy transition management should be carried out with the aforementioned objectives in mind. All these problems can contain many aspects, including ability to maintain indicators of security, stability and resilience (SSR). The problem of security of energy supply includes a known issue of preventing large-scale blackouts. However, during the period of energy transition, this problem becomes especially acute, because development of intermittent RE generation can lead to a decrease in the stability of electrical networks due to a decrease in the levels of inertia of the system caused by the decommissioning of large synchronous generators and their replacement with energy sources of asynchronous nature. The inertia deficiency subsequently brings power system frequency stability problems. The possibility of major accidents cannot be completely ruled out. Additional request to development planning arises: the power system must be able to minimize the consequences of extreme weather or malicious physical or cyber-attacks. Or in another words, power system must be secure, stable and resilient.

The challenge of ensuring SSR can be divided into two interrelated tasks:

1. The task of long-term energy SSR, which is mainly associated with investments to maintain the energy balance in accordance with long-term plans for economic carbon net zero development.

2. The task of ensuring short-term SSR, focused on the ability to quickly respond to sudden deviations in the balance of generation and demand for electricity.

The issue of significant decrease of inertia levels in synchronous power systems has become a widely acknowledged issue concerning even power systems/synchronous areas with historically sufficient inertia levels and stability reserves, such as ENTSO-E and Nordic synchronous power systems [4] [5]. The expected decline in the system inertia is expected to worsen the frequency stability of the power systems and to amplify the defined SSR challenges forcing the power system operators to seek countermeasures and to redefine system operation philosophies. This is especially true for smaller/islanded synchronous power systems as f.ex. Ireland or the Baltic states operating in an island mode after their desynchronization from the UPS/IPS power system in 2025 [6].

One of the most popular and discussed measures to counteract the decrease of the share of synchronous generators and power grids and thus the decrease in the inertia level – is introduction of synchronous condensers (SC) into the power system [7] [8] [9] [10]. The well-proven and known technology of SC relieves power system operators and helps to maintain sufficient inertia and short-circuit ratio levels independent of the dispatch pattern of the power generators. With the decreasing size of a power system – the introduction of SC increases in importance for the frequency stability of the power system.

A main topic of this thesis is the novel usage of a SC as an active power sensor to trigger rapid load shedding (LS) in order to quickly stabilize power system frequency in low-inertia power system conditions. As very well suited for islanded/smaller power systems this approach is to be proved to be extremely well suited for the Baltic synchronous power system operating in an island mode after their desynchronization from the UPS/IPS power system.

Implementation of the proposed solution has also a great fiscal potential to the socio-economic welfare (SEW) of the users of the Baltic power grid. Demonstrating the positive technical and financial gains of the proposed LS scheme with SC as a frequency sensor is going be the main contribution of this doctoral thesis.

No other literature is known to describe the scheme proposed in this thesis, also indirectly. The thesis is therefore assumed to propose a unique solution to a known and well-described power system issue.

This work fits into the international research of topic power system frequency stability.

The hypothesis, objective and tasks of the thesis

The hypothesis of the thesis: a load-shedding scheme based on the usage of SC as a frequency sensor substantially improves the frequency stability and increases the SEW for the grid users in a low-inertia power system.

The objective of the thesis: to prove that a load-shedding scheme based on the usage of SC as a frequency sensor has a major positive technical and fiscal effect on the Baltic synchronous power system operating in an island mode after their desynchronization from the UPS/IPS power system.

The tasks of the thesis:
1) introduce and describe theoretical and practical aspects of a novel LS scheme using a SC as a frequency sensor
2) through power grid simulations prove that the described LS scheme improves the frequency stability
3) through power market simulations and analysis that the described LS scheme has a major fiscal effect on the Baltic synchronous power system operating in an island mode after their desynchronization from the UPS/IPS power system

Research methods and tools

1) For dynamic power system frequency simulations the SIEMENS PSSE ver. 34 grid simulation software was used (under the license provided by the Latvian TSO AS Augstsprieguma Tikls).
2) For power system transient stability simulations ETAP 12.5 grid simulation software was used (under the license provided by the Riga Technical University).
3) The SEW analysis were conducted using the EUPHEMIA algorithm simulation tool Simulation Facility (under the license provided by the Latvian TSO AS Augstsprieguma Tikls).

Scientific novelty

The scientific novelty of the research presented in this thesis can be summarized by the following points:

1) A unique and novel LS scheme based on usage of SC as a frequency sensor
2) Dynamic frequency stability simulations of an islanded low-inertia synchronous power system with SC present, with and without the proposed novel LS scheme
3) SEW simulations/analysis showing the financial effect of the proposed novel LS scheme for an islanded low-inertia synchronous power system

Practical significance of the research

The work carried out during the development of this thesis as well as its results have contributed to a number of research projects:

- The Latvian Council of Science project "*Management and Operation of an Intelligent Power System (I-POWER)*" (2018–2021);
- National Research Programme "*Energy*" project "*Innovative smart grid technologies and their optimization (INGRIDO)*" (2018–2021);
- National Research Programme "*Energy*" project "*Future-proof development of the Latvian power system in an integrated Europe (FutureProof)*" (2018–2021);

Author's personal contribution

The idea and the concept of a LS scheme based on the usage of SC as a frequency sensor was developed together with Prof. A. Sauhats.

The work on proving the concept to be effective and technically viable was carried through a series of dynamic frequency stability simulations of the islanded Baltic power system in the SIEMENS PSSE ver. 34 grid simulation software. These simulations required a viable Baltic grid model, the work on the grid model and the simulations was carried out in close cooperation with M.Sc. J. Silinevics (AS Augstsprieguma Tikls).

The work on the analysis of the SEW contribution if applying the proposed LS scheme in the islanded Baltic power system was carried through:

- a socio-economic welfare simulation using the EUPHEMIA algorithm simulation tool Simulation Facility in close cooperation with Dr. A. Lvovs and Dr. G. Junghans (both from AS Augstsprieguma Tikls)

- a socio-economic welfare simulation using the Riga Technical University in-house simulation tool in close cooperation with Dr. R. Petricenko and Prof. A. Sauhats.

Approbation of the results

The research results included in this doctoral thesis have been presented in the following international scientific conferences/competitions:

1. MEDPOWER 2020 – Mediterranean Conference on Power Generation, Transmission, Distribution and Energy Conversion, November 9-12, 2020, Paphos, Cyprus.
2. 61th International Scientific Conference on Power and Electrical Engineering of Riga Technical University (RTUCON), November 5-7, 2020, Riga, Latvia.
3. 31st European Safety and Reliability Conference, ESREL 2021, September 19-23, 2021, Angers, France.
4. 60th ESReDA Seminar: Advances in Modelling to Improve Network Resilience, May 4-5, 2022, Grenoble, France.
5. 2023 IEEE PES Grid Edge Technologies Conference, Ph.D. Dissertation Challenge, April 10-13, 2023, San Diego, U.S.A.
(https://drive.google.com/file/d/1IRCGOdnmsmj3w5RGrK--LSAmUKXlakaG/view?usp=sharing)

The results included in this thesis have been published in the following <u>peer-reviewed scientific publications</u> (indexing in Scopus/Web of Science (WoS) indicated in parenthesis):

1. **D. Guzs,** A. Utans, A. Sauhats, G. Junghans and J. Silinevics, "Resilience of the Baltic power system when operating in island mode", 2020 IEEE 61th International Scientific Conference on Power and Electrical Engineering of Riga Technical University (RTUCON), Riga, Latvia, 2020, pp. 1-6, doi: 10.1109/RTUCON51174.2020.9316616.
2. Sauhats A., Utans A., Silinevics J., Junghans G., **Guzs D.**, "Enhancing power system frequency with a novel load shedding method including monitoring of synchronous condensers' power injections", 2021 Energies, 14 (5), art. no. 1490, DOI: 10.3390/en14051490
3. **Guzs D.,** Utans A., Sauhats A., "Evaluation of the resilience of the Baltic power system when operating in island mode", Proceedings of the 31st European Safety and Reliability Conference, ESREL 2021, pp. 1876 - 1883, DOI: 10.3850/978-981-18-2016-8_056-cd
4. Utans A., Sauhats A., Zemite L., **Guzs D.**, "Improving Power System Frequency Response with a Novel Load Shedding Method", 60th ESReDA Seminar: Advances in Modelling to Improve Network Resilience, France, Grenoble, May 4-5, 2022. Grenoble, France, pp.1-6.
5. **D. Guzs,** A. Utans, A. Sauhats, G. Junghans and J. Silinevics, "Resilience of the Baltic Power System When Operating in Island Mode," IEEE Transactions on Industry Applications, vol. 58, no. 3, pp. 3175-3183, May-June 2022, doi: 10.1109/TIA.2022.3152714**.**

Volume and structure of the thesis

The doctoral thesis is written in English. It is composed of introduction, six main chapters, 21 second-level subchapters, 21 third-level subchapters, conclusions and a bibliography with 97 references. The thesis also contains 31 figures and 19 tables. The volume of the thesis is 92 pages.

<u>Chapter 1</u> is dedicated to theory and background information on power system inertia, frequency, synchronous condensers, load shedding schemes and the existing situation in the

Baltic power system as well as the expected future developments regarding the synchronization of Baltics to the ENTSO-E grid in 2025.

Chapter 2 proposes the concept and methods for a novel load shedding scheme using synchronous condensers as frequency/ROCOF sensors. Further, the methods for evaluating the socio-economic welfare gains of introducing this novel load shedding scheme are extensively described: both for the Euphemia model (historic data for year 2020) and for the in-house RTU power market model using forecast data for the future years 2030-2050.

Chapter 3 describes a set of simulation test cases where frequency stability of the modelled Baltic power system is assessed during large loss-of-generation contingencies. The two different test case sets use two different models of the Baltics but both give comprehensive results on the possible effect of the proposed load shedding scheme on the system frequency.

Chapter 4 describes a set of test cases where the potential effect of the proposed load shedding scheme on the socio-economic welfare gains is studied on a model using historical Baltic power market data for the year 2020.

Chapter 5 describes a set of test cases where the potential effect of the proposed load shedding scheme on the socio-economic welfare gains is studied on a model using forecasted Baltic power market data for the years 2030, 2040 and 2050.

Chapter 6 contains the discussion of the results of all the simulations, both for the frequency stability and for the socio-economic welfare.

Finally, the overall conclusions are made in the Conclusions.

1. THEORETICAL BACKGROUND AND LITERATURE STUDY

1.1. Power system inertia and inertial response

Frequency stability of alternating current (AC) power systems, together with the voltage and the transient angular stabilities, is a cornerstone of secure and reliable operation of any modern power system. Keeping the frequency at the nominal value of 50/60 Hz (depending on the region) is a complex exercise requiring a whole range of technical measures and management processes implemented and supervised by the transmission system operators (TSO). The ultimate goal of this complex of measures is to ensure that any disturbance or frequency deviation in the controlled AC power grid is met with adequate and timely countermeasures which ensure always keeping the frequency deviations within an acceptable range.

The fundamental relation between the active power balance and the frequency of the power system is derived from the swing equation, see eq. (1.1) [11].

$$\frac{df}{dt} = \Delta P \frac{f_{syn}}{2H_{tot}} \qquad (1.1)$$

The swing eq. states that the rate of change of the system frequency (ROCOF) is directly proportional to the instant active power imbalance ΔP of the system and is inverse proportional to the total system inertia H_{tot}. This means that in case of an instant outage of a power source as for example a power generation unit (generator) and an unchanged system load, an instant active power imbalance occurs, and the system frequency will start to fall with a ROCOF proportional to the amount of active power lost and inverse proportional to the system inertia. In a real multi-machine power system the system frequency at this very moment of the transient power imbalance oscillations alters from being a global to a local parameter [12] and the eq. (1.1) starts to describe the behavior of each generator separately. In this situation every synchronous electrical machine connected to the power grid will yield an inertial response – that is it will react locally to this negative ROCOF according to the same eq. (1.1) by injecting active electrical power obtained from transforming the mechanical power of its rotor (slowing the rotor down). This inertial response will restrict the fall of the frequency allowing to win time for the primary, secondary and tertiary frequency reserve mechanisms (also known as FCR, FRR and RR) to be activated in order to stabilize the system frequency. The different responses in the described generator outage situation are well depicted by Figure 1.1. Figure 1.2 shows the hierarchy of the frequency regulation/reserve mechanisms in AC power systems.
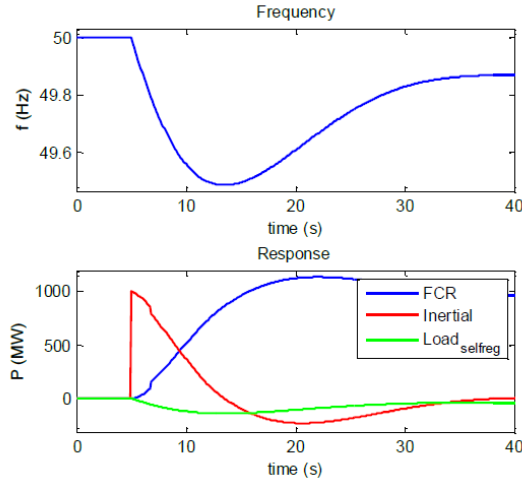
Figure 1.1. Frequency, inertial and FCR response to a generator outage [5]
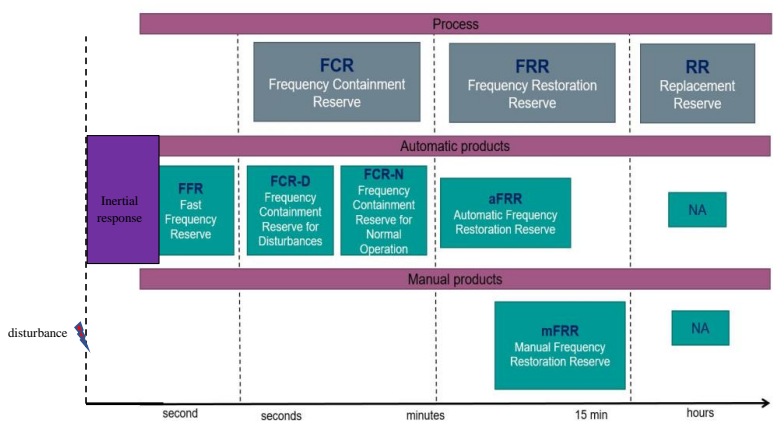
Figure 1.2. Frequency regulation reserve hierarchy in an AC power system

The Figure 1.1 clearly shows the importance of the inertial response of the synchronous electrical machines in the power grid: the inertial response is instant as it is a natural physical reaction of a synchronous machine to the frequency change. Without the inertial response the system frequency would have fallen much faster even before the FCR would manage to react and compensate for the frequency decline. This development would have led to frequency falling below an acceptable threshold causing cascading disconnections of the synchronous generators in the power system and thus a system-wide blackout.

The importance of the inertial response and the system inertia for the frequency stability becomes especially visible with the ongoing trend of decommissioning of conventional power sources and replacement of these with renewable and non-synchronous power sources. This

leads to a decrease in the overall power system inertia levels and thus to larger frequency deviations/ROCOF, as indicated by eq.(1.1), during incidents causing more frequency reserves to be consumed or in some cases – even load shedding (LS) schemes – to be activated. This forces system operators to look for alternative measures to sustain system inertia levels, as for example installation of synchronous condensers (SC) or synthetic inertia units [5] [13].

1.1.1. Challenges of timely detection of ROCOF

It is important to understand that the inertial response of the synchronous electrical machines in the power system is proportional to the *df/dt* (ROCOF), while the response of the primary frequency reserve (FCR) is only proportional to the *df*. The instant reaction time of the inertial response is a consequence of the "organicity" of the reaction of rotors in synchronous generators to the fluctuations in the grid (stator) frequency originating from the electromagnetic coupling between the rotor and the stator of a synchronous machine. Other possible corrective measures for rapid power system frequency stabilization such as synthetic inertia, fast frequency reserves (FFR, see Figure 1.2) or any advanced LS scheme have no other choice as to use ROCOF as an input exactly due the reason of rapidity of the ROCOF response and its unwavering connection with the active power balance of the power system. But as the above-mentioned frequency corrective measures lack the synchronous nature of a synchronous machine, these measures have to rely on a ROCOF measurement instead of a natural ΔP-ROCOF response. This fact emphasizes the importance of reliable and rapid ROCOF measurements. But securing both reliable and rapid ROCOF measurement is a challenging task.

The most common technique for ROCOF measurements is the measurement of time period between zero crossings of the voltage sinusoidal: the time period between zero crossings is translated into frequency and subsequent zero-crossing time periods are continuously compared to each other in order to detect the ROCOF. As this technique uses voltage sinusoidal measurement as input, it must be robust and resilient against grid voltage transients which are not caused by changes in the grids active power balance – for example voltage transients caused by transmission line short-circuits, grid switching operations, power electronics operations etc. These voltage transients introduce phase shift in the zero crossings of the voltage sinusoidal and can therefore disrupt frequency/ROCOF measurement quality, see Figure 1.3. The apparent way of avoiding the transient induced measurement disruptions, that is to distinguish between a real ROCOF incident and a grid fault or switching event induced transients, is to measure the zero crossing for more cycles thus ensuring the quality of the frequency/ROCOF measurement. Typical measuring window for a ROCOF measurement therefore is 2 – 100 cycles (40 ms – 2 s) [13]. In addition, a time delay of typically 50 – 500 ms is also introduced in order to avoid possible transients in the signal [13]. These numbers give us a very minimum time of no less than 100 ms for a ROCOF measurement – this measurement will be of low quality. Literature indicates 500 ms (0.5 s) to be an appropriate measurement period for a reliable ROCOF measurement [13].

Another argument against too quick ROCOF measurements are the damped frequency swings coming from real synchronous generators and their control systems following a power

imbalance incident in a real multi-machine AC power system. As every synchronous generator is a unique electrical machine with its own dynamic characteristics and control systems such as turbine governor, each generator will react with a different response to the frequency swing and to the following system load-flow change in a case of an incident. The load-flow change will alter the power angles on the transmission lines and therefore also force the remaining synchronous generators to change their angles. This will cause the overall system frequency to transiently swing in a damped manner before reaching a steady change tangent, see Figure 1.4. Thus a premature ROCOF measurement may also be biased by the transient frequency swings. As seen from Figure 1.4, 500 ms (0.5 s) is considered to be an appropriate measurement period for a reliable ROCOF measurement [13], while the standard measurement window for the frequency itself is 100 ms (0.1 s) or 5 full cycles in the 50 Hz grid [14].
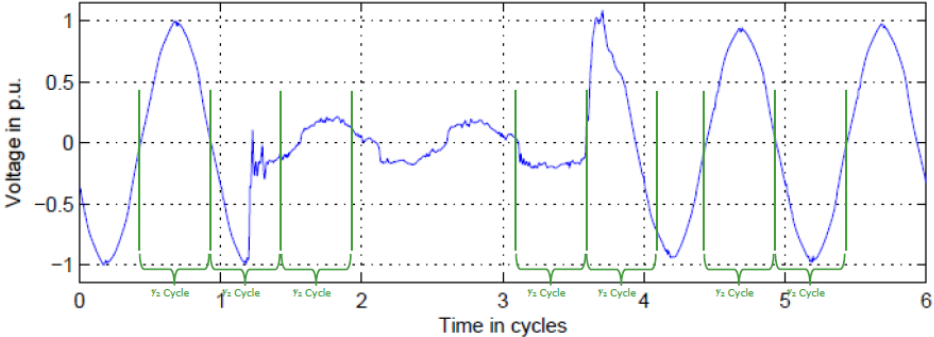
Figure 1.3 Zero crossings during a voltage transient [13]
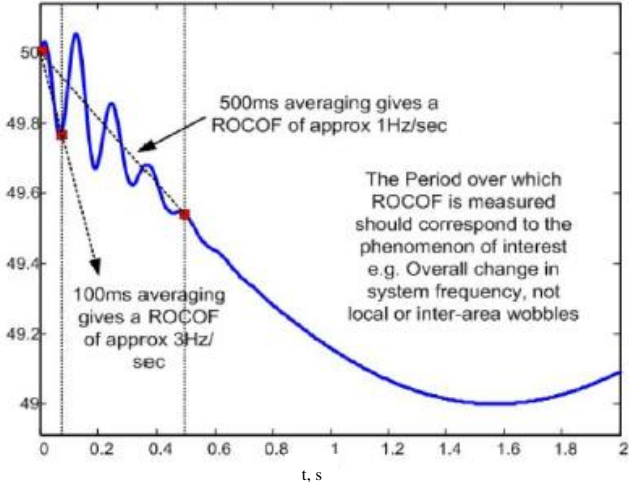
Figure 1.4. Frequency swings following a power imbalance incident [13]

21

1.2. Synchronous condensers

Synchronous condenser (SC) is a synchronous electrical machine which is not connected to any prime mover such as a steam or a hydro turbine. SC is neither a generator or a motor – as it does not produce or consume active power – but a synchronous electrical machine idling synchronously locked with the rotating electric field of the power grid. SC is basically an idling synchronous generator/motor and it behaves exactly the same way a synchronous generator does in terms of inertial or any other parameter response. A SC has all qualities of a classic synchronous generator, similar design and behavior. SC provides a wide reactive power regulating envelope, large short-circuit current capabilities and rotational inertia which can be additionally increased by means of installing a flywheel on the SC rotor shaft [15]. The inertia contribution of SC is a key feature considering the massive developments of renewable and non-synchronous sources and loss of system inertia. Literature considers installation of SC to be the best suitable technology for mitigating the reduction of power system inertia [13].

There has been a renewed interest in the industry for the use of SC [16] due to the already mentioned developments of the renewable energy sources un the reduction of the overall inertia levels of the AC power grids. SC have proved themselves well to enhance systems' frequency response [7] [10] as well as the systems' short-circuit capabilities [8]. Literature clearly shows the ability of SC to limit the negative ROCOF of the system frequency during a power-loss incident, see Figure 1.5.
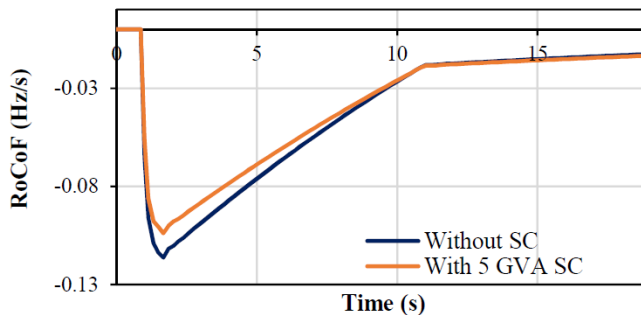
Figure 1.5. ROCOF comparison for an arbitrary system during a power-loss incident with and without SC [10]

1.3. Load shedding schemes in synchronous power systems

1.3.1. Traditional under-frequency load shedding (UFLS)

Under-frequency load shedding (UFLS) is a classic and commonly accepted measure used in AC power systems to counteract a potential frequency collapse following a serious loss-of-generation incidents and instant imbalance between generated and consumed power. The UFLS is typically triggered when the activation of available frequency reserves does not provide a sufficient frequency stabilization. UFLS is usually defined by a list of loads with matching frequency thresholds which are disconnected from the grid by frequency relays when the grid

frequency reaches any of the predetermined thresholds in the list. The use of UFLS obeys the eq. (1.1) – it reduces the ΔP and thus improves the ROCOF of the power system, or even switches the ROCOF from negative to positive contributing to stabilize the system frequency. The loads disconnected by UFLS are typically the whole MV side/-s of a HV/MV substation/-s [17]. The schematic logic principle of UFLS can be seen in Figure 1.6.
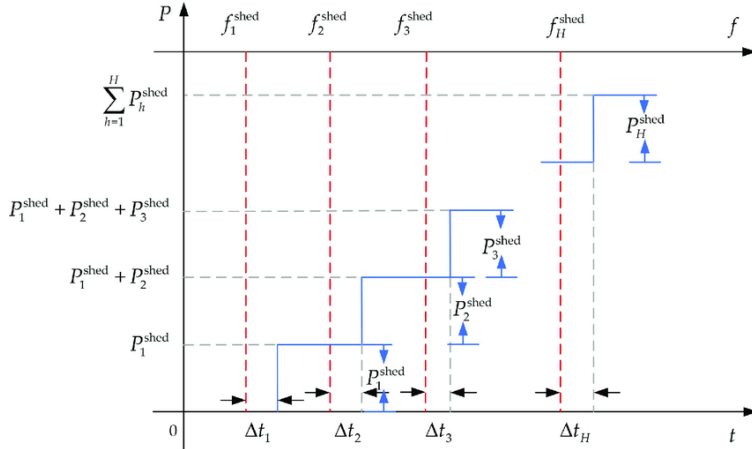
Figure 1.6. Logic principle of traditional UFLS [18]

A classical UFLS has several steps of load disconnection and frequency thresholds and the amount of load disconnected for each step is predefined but may differ from system to system depending on the system specifics. The main disadvantage of such "static" UFLS schemes is their inability to adapt fixed thresholds and the amount of load to be shed by each step to continuously varying load/generation profiles and to severity of power imbalance. These deficiencies may result in late response or excessive load shedding. It is a common understanding that for the load-shedding to be effective it should be activated as quickly as possible and simultaneously it should be resilient to small disturbances so that no excessive load is shed [19].

The importance of UFLS and of its response time increases with decreasing power system size and inertia as the UFLS frequency thresholds are reached faster in smaller AC power systems with less inertia. An introduction of faster UFLS triggering would therefore be beneficial especially for AC systems of medium and small sizes – due to smaller time margins before the frequency reaches critical values in those AC systems.

1.3.2. Advanced load shedding schemes

Traditional UFLS schemes – triggered solely by a frequency threshold – can be enhanced by more sophisticated UFLS schemes and concepts proposed and described in the literature [19] [20] [21] [22] [23]. A semi-adaptive UFLS scheme can use a triggering method utilizing static frequency and ROCOF thresholds instead of a frequency-only approach. An adaptive

UFLS scheme can adopt triggering methods employing a dynamic combination of frequency and ROCOF. Another type of dynamic UFLS schemes use algorithms including calculating the system inertia values or the total power imbalance of the system and use these for load shedding triggering together with frequency and ROCOF threshold values [21] [22] or even bus voltage threshold values [23]. Some of the adaptive schemes described by the literature propose to use artificial intelligence or neural networks in order to automatically determine the number of loads to be shed for each disturbance, but it is unclear how to educate the neural network without compromising the safety and stability of a real power system [24]. All the proposed UFLS schemes use frequency measurements in one or another manner.

Despite the advantages of the adaptive approaches over the classic one, the disadvantages of the adaptive UFLS schemes are well known and described [25]. A still ongoing search for new methods or concepts for UFLS is explained by the complexity of using eq. (1.1) in adaptive approaches due to the complexity of a real power system with many generators, each with own moment of inertia. The frequency in a multi-machine power system becomes a local parameter during the transient power imbalance oscillations and the eq. (1.1) is then describing the behavior of each generator separately. As a result, to estimate the disturbance ΔP, knowledge of the frequencies and inertia of many generators in the power system is required. This fact indicates that a predictive approach to UFLS, as anticipated in [25], could be the next step in the development of UFLS. A search for improved UFLS approach for low-inertia power systems is the main motivation for this thesis and therefore a novel type of a predictive LS algorithm will be presented by the author.

1.3.3. Economic rationality of UFLS schemes

The fundamental need for a UFLS scheme is dictated by the economic rationality behind the historically increasing size of generation units in the power systems. The historical growth of power generation units progressed in order to reduce the cost per unit of generated electrical energy, as increase in size comes with an increase in economic efficiency of the production – a fundamental postulate of basic economic theory. Increased generator size also brings larger potential loss-of-generation incidents and subsequent larger drops in the system frequency. This provides the explanation of the economic rationality behind any UFLS system – UFLS system enables the power system to include large generation assets as larger loss-of-generation incidents can be tolerated with the UFLS present, thus UFLS scheme contributes to reduce the overall costs per unit of electrical energy. Indeed, a power system can also be built without a LS scheme, but this kind of system will remain economically suboptimal due to restricted maximums size of the generation units or an increased need for reserve capacity [14]. The economical suboptimality of a power system due to restricted maximum size of generation assets or sources is also the central topic of this paper – projected onto the expected developments in the Baltic power system after year 2025. The assessment of the socioeconomic costs expected as a result of this suboptimality is one of the goals of the thesis.

The literature study has shown that despite a rich selection of technical papers on UFLS and its variations almost no attention is devoted to the economic assessment of the impact of UFLS

schemes. This can be explained by the fact that UFLS is meant to serve as a last-resort measure to avoid a full frequency collapse/blackout and therefore is activated extremely seldom in large power systems or because it is anticipated that LS is anyway a more preferable alternative to a blackout and hence the costs of LS are to be considered to be justified no matter how high they are. Some scarce information on the cost of energy not served (ENS) of shed loads can be gained from authors from developing countries where LS is not a frequency stability countermeasure but rather a common measure to balance generation and load in an environment with chronical generation capacity scarcity. These numbers are anyway not relevant for our article as costs of ENS are specific to each country or region. In general authors of UFLS related scientific articles are focusing only on the improvement of the frequency stability of the power systems without understanding what costs UFLS schemes bring and what costs do these help to avoid. Cost of disconnected load always has a value – whether it is the value of lost load (VOLL) or value of ENS and differs for different types of loads (for example industrial, commercial or residential) and also from country to country. An activation of UFLS brings VOLL/ENS-related costs. On the other hand – by not using an UFLS scheme the power system risks a frequency collapse and a blackout bringing tremendous costs to the society. The available literature provides no traces of economic assessment of costs and benefits related to the presence of UFLS versus absence of UFLS in power systems.

When a LS scheme is activated loads are disconnected from the grid. The negative effect of load disconnection has been quantified in monetary terms by estimating the VOLL. In a power system a balance between the level of supply security and the costs must be maintained in order to maximize the socioeconomic welfare for the power consumers. The value of lost load describes the marginal benefit of additional security of supply and measures the loss of socioeconomic activity resulting from a unit of electric power not supplied by the grid [26]. This value will differ from region to region due to different median income and overall wealth, and will differ between the consumer types as some consumers are more price sensitive to the loss of the electric power supply than other consumers. [26] provides a good overview of the VOLL-values for different countries/regions in the EU and for different consumer types.

1.4. Wholesale day-ahead power market

The wholesale day-ahead power markets in the European Union (EU) are all based on the price formation logic called marginal price logic. The principle of this logic is as follows. The power exchanges, also known as Nominated Electricity Market Operators (NEMO), daily receive sell and buy bids from the respective generators and consumers in their market zone for each hour of the next day. NEMOs aggregate those bids and thus create a single cumulative row of bids for generation and consumption for each hour. A cumulative generation bid row grouped after the raising marginal price of the submitted bids is called for "merit-order" as it orders the available submitted generation after the price for which the sellers/generators are willing to sell their power for [27]. When for a given hour the consumption and generation cumulative bid curves intersect, as seen in the Figure 1.7, the market cross is conceived. This market cross reveals what cumulative volume the consumers are ready to consume at a certain

marginal price at which the generators are ready to sell their generated power. The power price given by the market cross is the price of the last bids in both cumulative bid curves; this means the market cross price is the one all of the activated generation bids will receive (even if some of these have bidden at a lower price) hence the name of marginal price logic. The same principle applies to the consumers – all of the consumers will pay the same marginal price for the power even if some of the consumption bids were priced higher. The principle and logic of marginal power price provides a fair balance between the interests of power consumers and producers. The socioeconomic welfare provided by the marginal price power market model is the net sum of the extra income the generators receive (producer surplus) and the extra savings consumers harvest in comparison to what they were willing to buy/sell the power for according to their bids (consumer surplus) [28]. These surpluses of consumers and generators (producers) are illustrated by the red and blue areas in the Figure 1.7.

Despite a behavior typical to any other commodity markets, the power market has one special attribute – extreme inelasticity of the demand at the lower volumes. This is caused by the critical nature of the consumption of the electricity – some minimum electricity demand is so critical that it must be met at almost any cost. This fact can lead to extreme price values for the demand curve in the lower volume range and therefore power exchanges typically impose a max bid price cap in order to protect the market and the consumers from extreme price spikes. As an example, Nordpool – one of the major European NEMOs – has a max price cap of 4000 EUR/MWh [29]. This fact has also an important implication on the consumer surplus – the consumer surplus will be calculated taking into account the delta between the market price and the max price cap, and therefore potentially generating large numericals which can seem to be illogical or ridiculous. One has to remember that the power market consumer surplus does show the difference between the market price and the price the consumer is willing to pay for electric power, therefore the massive numbers of the consumer surplus reflect the extreme inelasticity of the electric power demand. The other-way-around situation with the massive power producers' surplus can also be the case when a lot of unflexible base load is present in the power system and must be sold at a nearly-zero price.

Since EU consists of many countries and market zones, all of these have to be coupled in between in order to achieve a pan-European market coupling and to enable cross-border power flows in accordance to the goal of maximization of the total socioeconomic welfare which is the sum of the consumer and producer surpluses. This common EU day-ahead power market coupling solution uses the Single Price Coupling Algorithm called Euphemia. Public description of Euphemia can be accessed in [30]. Euphemia solves the market coupling optimization problem consisting of supply and demand bids, considering limitations - cross-border capacities between bidding zone borders and allocation constraints. Optimization problem's goal is now to maximize the total socioeconomic welfare of the whole interconnected area and not a single market zone. This means that a net socioeconomic welfare of a single market zone can even theoretically be reduced in order to increase of the net total welfare of the interconnected area. As already mentioned the net socioeconomic welfare consists of the sum of consumer and producer surplus as shown by the Figure 1.7.
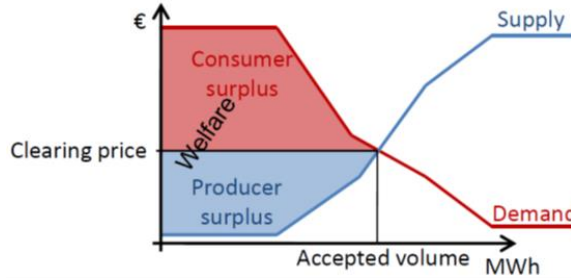
Figure 1.7. Price cross of the power supply and demand curves, graphic definition of socio-economic welfare [31]

1.5. Power system of the Baltic states

1.5.1. General information and planned ENTSO-E synchronization

Power transmission grid of the Baltic states is a meshed, interconnected 330 kV grid with a peak load of ca. 4000 MW [32]. It has a strong synchronous interconnection with the Unified Power System of Russia (UPS) synchronous power system and has asynchronous HVDC connections to both Finland, Sweden and Poland, see Figure 1.8. The maximum exchange capacity of all interconnections to the Baltics is around 4700 MW [14], which makes it theoretically possible to supply the peak load of Baltic power grid with imports alone. Main generation assets in the Baltic power grid comprise of thermal oil-shale and wind power generation in Estonia, large river hydro power plants plus a major gas-fired power plant (Riga TEC2) in Latvia and a combination of wind power, small/medium sized CHPs, a major pump-storage and a major gas-fired power plant in Lithuania. Baltic power grid is heavily relying on imported power with the total import comprising in 2019 47,6% of the total consumption, with largest net power exporters to the Baltics in 2019 being Belarus, Finland and Sweden [33].

The interconnection with UPS today provides the Baltic power system with vast frequency and inertia reserves. Frequency stability is not an issue in today's situation due to the size of the UPS synchronous power system. A political decision has been taken to desynchronize the Baltic states from the UPS power system and to synchronously connect it with the European Network of Transmission System Operators (ENTSO-E) power grid in 2025 [6]. This plan proposes the disconnection of the nine 330 kV transmission lines synchronously interconnecting the Baltic and the UPS power systems. These lines have a total thermal capacity of ca. 9000 MW and a nominal transmission capacity of ca. 2500 MW, see Figure 1.8. After the disconnection itself, a synchronous connection between the Baltic and the ENTSO-E (Poland) power systems is to be established through a single double-circuit 400 kV synchronous interconnection on the border Lithuania-Poland with thermal capacity of ca. 2000 MW [14].

In situations when this synchronous interconnector between Baltics and Poland goes out on a planned or an unplanned outage, the result will be the operation of Baltic states' power grid in an island mode. During this mode of operation the Baltic power system is only to rely on its

own inertia and frequency reserves which are radically lower than today's available inertia and frequency reserves provided by the UPS power grid. The island mode of operation is to introduce major challenges to the operational frequency stability of the Baltic power grid. The main and fundamental challenge the Baltic power system will face is the vast size of the generation/HVDC units compared to the overall size of the power system in the island mode. One must remember that all grid developments in the Baltic power system were done in a situation with an existing interconnection with the UPS system and thus only economic, rather than inertia- or frequency-related, optimums steered the dimensioning of both generators, loads and HVDC interconnectors [14]. This historical development resulted also in the lack of ability of the existing conventional power plants to provide a rapid frequency support – so much needed in the radically different island mode expected in the Baltic power system after the desynchronization – simply by the reason that this kind of technical ability was not needed.
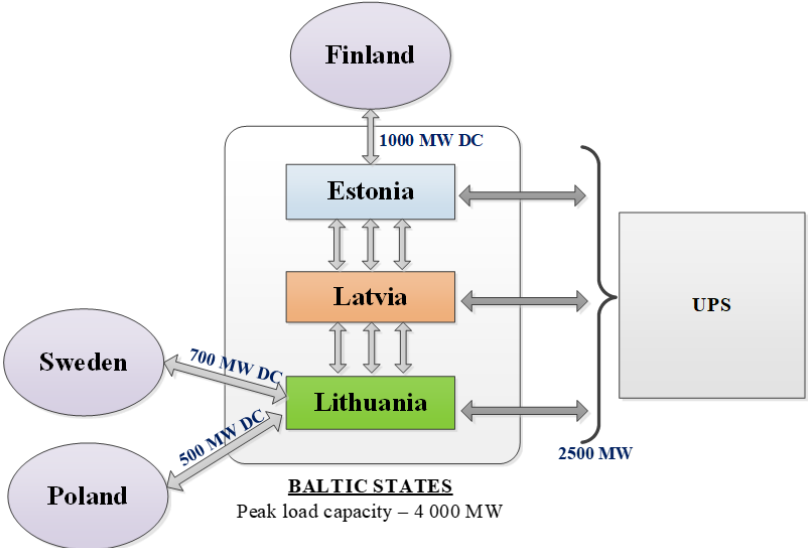
Figure 1.8. Schematic power system interconnection of the Baltic states.

Another development to impact the inertia level of the Baltic power system is the expected rise in intermittent non-synchronous renewable generation capacity. Around 4000 MW of wind generation capacity is planned in the Baltic states up to year 2034 according to [34]. Separate national renewable energy targets in the scope of the EU 2030 Climate & Energy Framework [35] indicate sharp rise of share of renewable generation in Estonia and Lithuania, while Latvia is already close to fulfilling 2030 renewable electricity targets due to large existing hydropower generation capacity [36] [37] [38]. RES are non-synchronous so they do not contribute to the system inertia. This implies that the total inertia level of the Baltic power system is expected to decline. It also expected that due to the rise of the share of intermittent generation and the subsequent volatility of the power prices, the operation of the synchronous generators is to be

more volatile, with more start-and-stop cycles [39]. This means also volatility in the level of the total inertia of the power system.

To mitigate these developments and to safeguard frequency stability of the Baltic power grid, the European and Baltic TSOs have agreed to implement a range of measures. One of these is to invest in three synchronous condensers (SC) rated ca. 305 MVA for each Baltic TSO each – totaling nine synchronous condensers planned in the Baltic power grid by 2025 [14]. The expected placement of these SC in the Baltic power grid can be seen in the Figure 1.9.
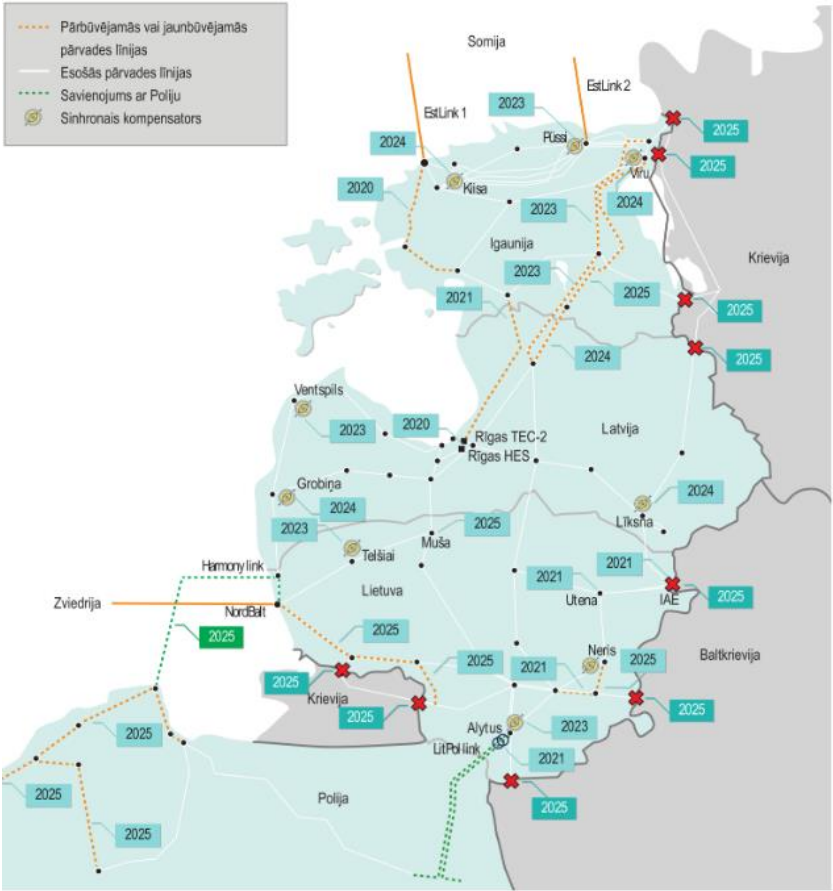
Figure 1.9. Baltic power system after desynchronization [40]

Another planned measure is to install battery storage systems for rapid FCR provision [40] [14], a move literature has anticipated earlier and even provided methods to implement with [41].

From the wholesale power market point of view, the Baltic states are fully integrated in the common EU power market. Estonian, Latvian and Lithuanian bidding zones are part of Single Day-ahead Coupling (SDAC), which involves 31 Transmission System Operators (TSOs) and 16 NEMOs. According to information of European Network of Transmission System Operators

(ENTSO-E), common market solution couples 95% of EU power consumption, i.e. one solution couples 1500TWh/year [42].

1.5.2. Existing UFLS scheme in the Baltic power system

As already mentioned in the Chapter 1.3.1 any AC power system has a UFLS scheme implemented for protection from a frequency breakdown. This is also the case for the Baltic power system working synchronously with the UPS power system. The parameters of the UFLS scheme of the Baltic power system can be seen in the Table 1.1.

Table 1.1. ULFS parameters in the Baltic power system [43]

The Baltic states UFLS system's operational parameters	Connected load to UFLS systems		
	Latvia	*Estonia*	*Lithuania*
The special UFLS stage, Fset. = 49.2 Hz, Tset. = 0.5 s	3.0%	3.0%	3.0%
Fset.$_{1-st\ stage}$ = 48.8 Hz, Tset. = 0.5 s	4.7%	4.7%	4.7%
Fset.$_{2-nd\ stage}$ = 48.6 Hz, Tset. = 0.5 s	4.7%	4.7%	4.7%
Fset.$_{3-rd\ stage}$ = 48.4 Hz, Tset. = 0.5 s	4.7%	4.7%	4.7%
Fset.$_{4-th\ stage}$ = 48.2 Hz, Tset. = 0.5 s	4.7%	4.7%	4.7%
Fset.$_{5-th\ stage}$ = 48.0 Hz, Tset. = 0.5 s	4.7%	4.7%	4.7%
Fset.$_{6-th\ stage}$ = 47.8 Hz, Tset. = 0.5 s	4.7%	4.7%	4.7%
Fset.$_{7-th\ stage}$ = 47.6 Hz, Tset. = 0.5 s	4.7%	4.7%	4.7%
Fset.$_{8-th\ stage}$ = 47.4 Hz, Tset. = 0.5 s	4.7%	4.7%	4.7%
Fset.$_{9-th\ stage}$ = 47.2 Hz, Tset. = 0.5 s	4.7%	4.7%	4.7%
Special and UFLS-1 system total:	45%	45%	45%
Non-combined UFLS-2 system, Fset.= 49.2 Hz, 2.3...2.7%/stage, Tset.= 10 / 15 / 20 / 25 s (4 stages)	10%	10%	10%
Combined UFLS-2 (part of UFLS-1), Fset. = 48.7 - 49.0 Hz, 4.5%/stage, Tset. = 30 / 40 / 50 / 60 / 70 / 80 s	27%	27%	27%
Total connected load to UFLS, UFLS-1 and UFLS-2 systems	55%	55%	55%

2. A NOVEL LOAD SHEDDING SCHEME – CONCEPT, MATERIALS AND METHODS, ECONOMIC RATIONALITY

2.1. Inertia and inertial response in real multi-machine AC power systems

Any power system under consideration includes following elements: synchronous generators, synchronous condensers, load with electric motors, renewable energy sources and high-voltage grid tie lines.

An unexpected disconnection of a large generator in the power system causes a transition to a new state – in particular, the rotation frequency of synchronous generators, synchronous condensers and motors is subject to change (decreases). In the process of decelerating of rotating masses of the elements of the power system, the kinetic energy accumulated in them is transformed into electric energy and injected into the electrical network. As result of this injection (inertial response) the balance of generated and consumed electrical energy is maintained even during the transient process. Within a few seconds delay after disturbance, generator's governors, in response to a decrease in frequency, start to react on the frequency decline trying to restore the frequency rated value (primary frequency control). Additionally, diminishing of the frequency causes a decrease in the power consumption of the frequency dependent load. However, the initial period of the considered transient process is mainly determined by the disconnected generator with active power ΔP at the beginning of the process and the inertia of the system. In such case the impact of primary frequency control and the decrease in the power consumption can be neglected. Consequently, we can assert that the volume of the disconnected power ΔP at the very beginning of the process prior to primary frequency control is compensated by the injection of the active power by each element of the power system possessing inertia:

$$\Delta P = \sum_{a=1}^{S} \Delta P_{SC\_a} + \sum_{b=1}^{G} \Delta P_{G\_b} + \sum_{c=1}^{L} \Delta P_{L\_c}, \ \forall a \in S, \ \forall b \in G, \ \forall c \in L \quad (2.1)$$

where ΔP_{SC_a}, ΔP_{G_b} and ΔP_{L_c} are active power injections of every synchronous condenser, synchronous generator and frequency dependent load (for example electric motors) present in the power grid; where S, G, L are the total numbers of synchronous condensers, synchronous generators and frequency dependent loads in the power grid. To stop the change in frequency, it is enough to restore the balance of generation and consumption by disconnecting, for example, a load equal to ΔP. Estimates of the volume of this load can be carried out on the basis of measuring all ΔP's included in eq. (2.1). However, in real power systems, due to the large number of elements, this path is unacceptable. The problem can be simplified by assuming that eq. (2.1) can be represented as:

$$\Delta P = K_r * \sum_{a=1}^{S} \Delta P_{SC\_a} \quad (2.2)$$

where $K_r = \dfrac{\sum_{b=1}^{G} \Delta P_{G\_b} + \sum_{c=1}^{L} \Delta P_{L\_c}}{\sum_{a=1}^{S} \Delta P_{SC\_a}} + 1$

If the coefficient K_r is known, to estimate ΔP it is sufficient to measure the power injections of all synchronous condensers $\sum \Delta P_{SC}$. In real life, the coefficient K_r is not a constant value, it depends on the operating mode of the power system, its topology and also of the total system inertia level. However, in any case, we can assert that the measured $\sum \Delta P_{SC}$ can be taken as the basis for disconnecting/shedding the load for frequency stabilization. This load shed must be in a volume not less than $\sum \Delta P_{SC}$. Such disconnection, as will be shown below, can significantly increase the efficiency of systems where the main source of inertia are synchronous condensers. Eq. (2.2) will give an opportunity to rapidly predict the fall in the system frequency and therefore form the basis of the decision to initiate a fast triggering of the proposed LS scheme. Monitoring of SCs only is achievable in practice and can be used as a basis for power imbalance and system frequency prediction. The implementation of such a concept would require usage of a Wide Area Measurement System and dedicated measurement units/terminals.

2.2. The concept of the proposed novel LS scheme

The simulations conducted for the Baltic grid in island mode [44] have shown that after shortfall of a major generation unit in the Baltics a ROCOF of 0.75 Hz/s (0–500 ms) is observed and the typical classic first UFLS threshold of 49 Hz is reached in approx. 1.75 s from the moment of the contingency. That means that if an alternative UFLS method is to bring added value to the Baltic power grid it should provide triggering considerably faster than 1.75 s. [45] states that a fast response for frequency stabilization should be activated faster than 800 ms in situations with ROCOF of around 1 Hz/s, and load shedding can be considered as a type of frequency stabilization measure.

This thesis would like to propose a novel LS concept – a concept using a principle of much faster triggering of LS than that of the conventional UFLS. This novel principle will allow to trigger (not to be confused with activate) LS not later than 100 ms from the moment of the contingency without usage of either frequency or ROCOF measurements. The triggering time is considerably faster than conventional UFLS because it is based on a predictive approach. The principle of this predictive approach is based on the monitoring of the active power injections of the SCs present in the power system. The rationale is following: active power injection of a SC in an AC power system contains information on the ROCOF of the system and according to the eq. (1.1) that corresponds to an instantaneous disbalance in the active power parity in the power system. SC active power injections can therefore be used as a set off for rapid LS activation. Execution of such a rapid scheme of LS substantially reduces the frequency fall and the value of frequency nadir, thus greatly reducing the risk of frequency limit violation in the given power grid. The schematic representation of the proposed novel LS principle is seen in Figure 2.1.
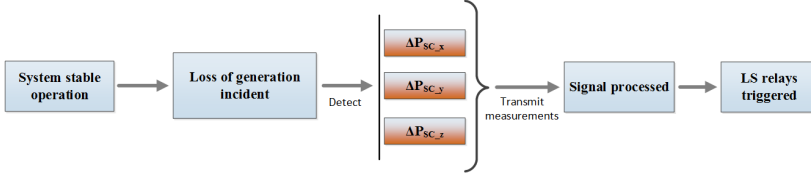
Figure 2.1. Schematic of the proposed novel LS principle.

To prove the concept and the hypothesis this thesis will conduct assessments for both frequency stability gains and socio-economic gains potentially delivered by introduction of the proposed novel LS scheme into a practical AC power system.

2.2.1. Technical details of the proposed novel LS scheme implementation

Several different automation concepts can be used to implement the proposed LS method in practice. The SC active power injection measurements can trigger a SCADA based LS algorithm which will calculate the amount of load-shedding needed and activate the load-shedding relays. The function of measuring the active power can be as-signed to the terminals of microprocessor based relay protection (for example as an addition to out-of-step protection automation) since these devices use active and reactive components of the vectors of currents and voltages: U_a, U_r and I_a, I_r [46] [47]. The measurements of this values at times t and t + 1 allow as to calculate the total active power injection based on elementary arithmetic operations according to eq. (2.3):

$$\Delta P(t+1) = U_{a(t+1)}I_{a(t+1)} + U_{r(t+1)}I_{r(t+1)} - (U_{a(t)}I_{a(t)} + U_{r(t)}I_{r(t)}) \qquad (2.3)$$

A potential scheme for the SC measurement arrangement can be seen in Figure 2.2.
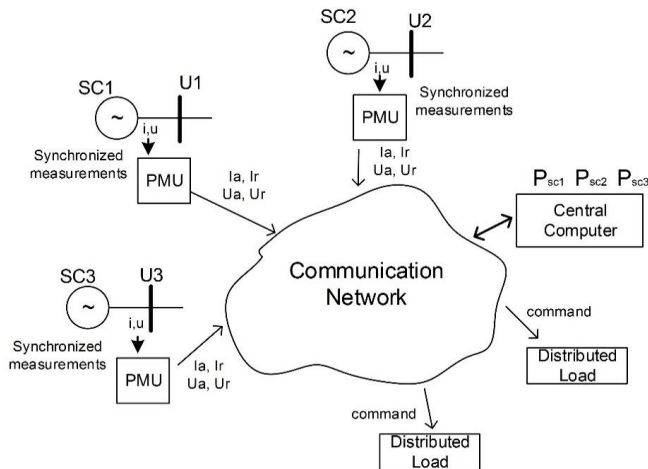
Figure 2.2. Potential measurement/command arrangement for the proposed LS scheme.

33

A flowchart of the proposed LS algorithm is presented in the Figure 2.3. The voltage and current phasors are collected from PMUs as in Figure 2.2, and to calculate the active power injection of the SC the eq. (2.3) is used. Load shedding sequence is triggered when a SC active power injection exceeds a certain minimum allowed imbalance value. At next step the amount of load to be shed is calculated. The final step is sending tripping commands to appropriate relays/IEDs according with calculated required shed load.
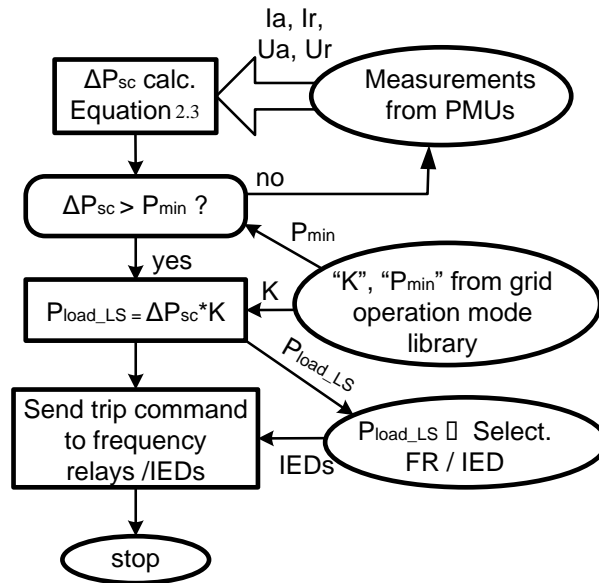
Figure 2.3. Potential LS scheme execution algorithm.

All in all, the proposed LS arrangement/scheme is assumed not to be challenging to implement in practical power grid as all the hardware components are serially available and they all, apart from the SC themselves, have negligible capital costs [14]. The software for the operation logics can be created in-house in the RTU/AS Augstsprieguma Tikls, as this kind of competence and experience is available in the named organizations [14].

2.3. Socio-economic motivation for the proposed novel LS scheme

Activation of LS schemes has traditionally been considered as measure triggered only by critical grid situations (mostly frequency contingencies), considered a measure subjected purely to technical considerations and not to any sort of economic or socioeconomic examination. This thesis will angle a different view on the usage of LS, a view where LS is examined also from socioeconomic angle, where a quantification is given not only to the technical contribution of the LS scheme (eg. frequency support) but also a to its socio-economic beneficence. In this manner LS can be looked at as a sort of ultra-rapid reserve, which can also be provided on commercial terms by flexible consumers and thus provide a base for an another type of auxiliary

service market operated by the TSOs. This kind of auxiliary service of ultra-rapid reserve can provide TSOs with possibilities of introducing less stringent N-1 grid security criteria (both for generation and transmission assets) and so increasing transmission capacities between bidding zones/market areas, thus potentially lowering the socio-economic costs and increasing socio-economic welfare in these areas. [48] provides a methodology on the assessment of the socio-economic costs connected to the transmission capacities and the interruption costs similar to those arising from LS scheme activation. The methodology used in this thesis will be similar to the one used in [48] but adjusted for the details of the case study of the thesis, which is the Baltic States' power system after the planned synchronization with the ENTSO-E area in 2025.

As mentioned, after the synchronization with the ENTSO-E in 2025 the power system of the Baltics will have only one double-circuit 400 kV synchronous interconnection with the rest of the ENTSO-E (Poland). The available transmission capacity on this AC link is planned to be only 100 MW [14]. Any common-mode outage of this line will lead to an islanding of the Baltic power system, a mode of operation with major challenges to the frequency stability of the Baltic power grid. The expected reduction of the system inertia levels due to the rising share of non-synchronous renewable generation capacity in the Baltics additionally severely worsens the frequency stability outlook of the post-2025 Baltic power system in the island mode.

In addition to the already mentioned installation of the SC in the Baltic power system, another mitigation is planned for the island mode of operation – market restrictions. The following market-based actions are to be instantly carried out in the Baltic power grid in the case of the event of island operation [14]:

- Immediate reduction of the transmission capacities on the importing HVDC connections down to max. 400 MW import capacity
- Following redispatch of the power plants/activation of reserves as result of these HVDC capacity restrictions

These restrictions are to ensure that a no single power source delivers more than 400 MW of active power into the Baltic power grid. 400 MW is an amount the Baltic TSOs consider to be a maximum safe limit for an outage incident the Baltic power system in island mode can withstand [14]. The restrictions are to be upheld as long as the islanding of the Baltic power system is in place. These island mode market restrictions of the import capacity into the Baltics are expected to result into a major reduction of the socioeconomic welfare, this mainly due to a lower supply volume available for the power market due to such import constraints. Additional costs for redispatch/extra activated power reserves and revenues from the inter-TSO border congestion fees also have to be taken into account during the island mode of operation market restrictions.

Power system of the Baltic states post year 2025 will be in a unique situation not present anywhere else in the world: a fully-sized AC power system synchronized with another large power system but always in the standby to go over into island mode of operation. This implies also a more probable activation of the LS scheme in the Baltic power system. The novel LS concept proposed by the thesis will prove in chapter 3 its effectiveness to maintain Baltic power system frequency stability in the island mode. Thus the proposed novel LS concept can result in the unnecessity of implementation of the mentioned market restrictions (single power source

delivers no more than 400 MW) during an event of islanding of the Baltic power system. This fact leads echoes the pronounced hypothesis and claims following: the proposed novel LS scheme may prevent a reduction of the socioeconomic welfare during the island mode of operation and therefore bring a substantial socioeconomic benefit to the Baltic states. An analysis/case study will be presented in chapter 4. The to-be-presented case study may also serve as a benchmark for socioeconomic welfare assessments of LS schemes for other constantly or variably islanded power systems.

2.4. Materials and methods for the socio-economic analysis

To investigate the proposed hypothesis about the increase of the SEW due to the proposed novel LS scheme, possible island operation modes of the Baltic power system shall be estimated, as well as the changes of socio-economic welfare, the gains from congestion income, the costs of power system reserve activation shall be analyzed and the consumer losses due to the load shedding shall be evaluated.

Island operation mode of the Baltic power system occurs in cases when there is an outage of the only synchronous interconnector between the Baltic States and the ENTSO-E area. Therefore, to estimate the loss to the SEW of the region, which would result from wholesale power market limitations during island mode operation, there is first of all a need to know how often and how long Baltic power systems would operate in an isolated mode. To estimate this, analysis of AC transmission line outage statistics is needed.

The reduction of socio-economic welfare – or the loss to the wholesale power market – occurs due to limited trading capacities on bidding-zone borders which could be introduced during the island operation mode. Simultaneously the TSOs are gaining increasing congestion income when capacities on bidding zone borders are being decreased. During the first hours of island mode operation – from the moment of the occurrence of the island operation mode till the moment the wholesale energy market takes into account the reduced trading capacities between bidding zones, the redispatch actions/emergency power reserves will be activated by TSOs to replace the reduced exchange capacities on the borders. During these hours there will be no reduction of socioeconomic welfare on the wholesale power market, but there will be costs to the TSO to operate the emergency power reserves.

Consumer losses due to the disconnections (VOLL/ENS) initiated by the proposed LS scheme will appear when major incidents, like tripping of HVDC cables, do occur explicitly during the island operation mode. Therefore, the statistics of probability of occurrence of major incidents are also needed, and these statistics will be ultimately cross-connected to the previously mentioned probability of Baltic power gird island mode operation. This ultimate probability of the major incident cross-connected with the probability of islanding of the Baltic power system and with the statistical data on VOLL costs will be used to estimate the final customer losses due to the proposed LS scheme.

The following subchapters of the chapter 2.4 will develop the methods for the assessment of the SEW of the test cases in the chapters 4 and 5.

2.4.1. Maximum permissible generation outage of the Baltic power system in island mode

Baltic TSOs have previously in their studies determined that a maximum allowed outage of a generation source for the Baltic system in island mode is an outage of no larger than 400 MW [14]. That is, a maximum generation outage the Baltic power system in island mode can withstand without violating the lowest permitted frequency limits and without activating the existent UFLS schemes. According to [14], the studies determining this maximum outage size were performed in 2016 and did not take account of the later decisions of the Baltic TSOs to install 9 SC in the Baltic power grid by 2025 as described in the chapter 1.5.

The thesis will verify the postulate of the maximum permissible outage of 400 MW by performing a dynamic simulation of a 400 MW generation outage on a model of the Baltic power system in island mode with 9 SC present in the grid. A sudden trip of a HVDC cable importing 400 MW in a typical Baltic winter power system mode was simulated and the frequency response was studied, see Figure 2.4. The active power results presented in the Figure 2.4 are scaled p.u. to the base MVA rating of 1200 MW, the frequency is scaled p.u. to the base of 50 Hz.
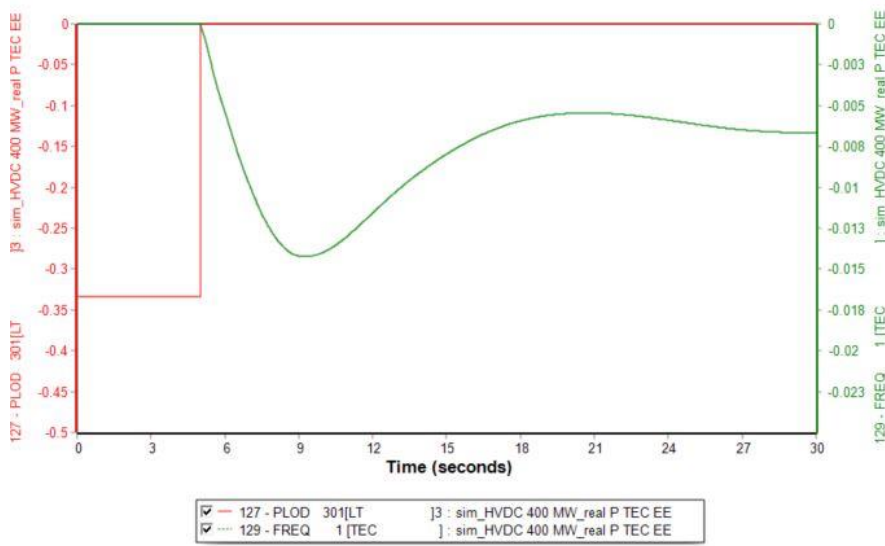
Figure 2.4. Frequency response of an islanded Baltic power system onto a 400 MW generation outage.

The simulation shows that a frequency nadir of 49.3 Hz is reached due to the outage, before the frequency stabilizes at 49.65 Hz. This result confirms the fact that no frequency collapse will take place due to a generation outage of 400 MW in island mode, but also casts doubt onto the postulate that 400 MW is the absolute maximum permissible generation outage for the Baltic power system in island mode as the absolute minimum instant permitted frequency value of 49 Hz was not reached during the simulation.

This finding may lead to that a maximum generation incident size may be reassessed by the Baltic TSOs or a dynamic maximum incident restriction may be introduced according to the power system modes, inertia level etc. This may also in the future lead to smaller market restrictions in case of the event of islanding of the Baltic power system.

2.4.2. Statistics of AC lines outages and major incidents

In the context of this paper, the main interest of AC line outage statistics is for the transmission line on the Lithuania-Poland border (LitPol Link), as the island operation mode of Baltic power system would occur in case of an outage of this line.

LitPol Link, for this case study, is understood not just as the one AC link between Lithuania and Poland, but is formed by two lines connected "in series" – one line from Alytus substation in Lithuania to Elk Bis substation in Poland, and the second line from Elk Bis substation to Lomza substation (also in Poland). Both lines should be taken into account as outage of any of them (both circuits) would mean loss of synchronous connection.

The operation of LitPol Link (the line between Alytus and Elk Bis substations) started at the end of 2015 [49] [50]. Based on the fact that this line is relatively new and only has been in operation for a relatively short period of time, the usage of available outage data, especially for common mode double circuit outages, taken directly from the LitPol link statistical data and extrapolated onto the future could be questionable. Therefore, usage of more credible data for the statistics of AC lines' outages is required and is by us taken from various sources regarding the outages of AC lines with voltages from 330kV till 500kV. Data on the number of outages per 100km of single-circuit AC line per year, as well as data on duration of outages (where available) has been gathered, as well as data on the outage probability ratio between single and double circuit (common mode) AC lines of the same voltage [51] [52] [53] [54] [55] [56]. This particular ratio is meant to be applied on the mentioned AC line statistics to deliver a universal number of common mode outage probability per 100 km of double-circuit line per year. These results are followingly applied to the LitPol Link by taking into account length of the whole link assumed in this paper. As a result there we get an estimated number for outages per year of the synchronous link between Baltic and ENTSO-E power systems and also the expected average outage duration, representing the expected regularity of the island operation mode and it's duration on a yearly basis.

When regarding the statistical data on the major incidents – the number of Baltic countries HVDC links' outages – it has been gathered from UMMs (urgent market messages) published on Nord Pool AS web page [57]. Data on the outages has been gathered per each HVDC link individually and for the whole time of the each link's operation. Then the average number of link's outages per year has been calculated as the gathered number of outages divided by the number of years the link is in operation. The sum of all HVDC links outage cases per year has been used in the paper as the number of major incidents, which directly affects the regularity of LS scheme activations and therefore also monetary losses faced by the consumers.

2.4.3. Methods of the test case' power market/power system simulations and the subsequent calculation of the SEW

To estimate the potential monetary gain of the proposed LS scheme, first of all, changes in the socioeconomic welfare of the Baltic wholesale electricity market/power system should be calculated for the cases without proposed LS scheme (and therefore – with restrictions to the cross-border transmission capacity) and then – with the proposed LS scheme (and hence with no cross-border capacity restrictions).

In order to assess this potential reduction of the socioeconomic welfare for the Baltic power system two different test case power market simulations will be conducted for this doctoral thesis:
- a simulation with historical data for 2020 using the Simulation facility tool
- a simulation set with forecasted data for 2030, 2040 and 2050 using an RTU-inhouse developed market simulation environment

- Simulation with historical data for 2020

As already described in the introduction, Baltic countries operate within the EU electricity market.

Figure 2.5 shows the geographical scope covered by the EU single coupled wholesale electricity day-ahead market (SDAC) [58].
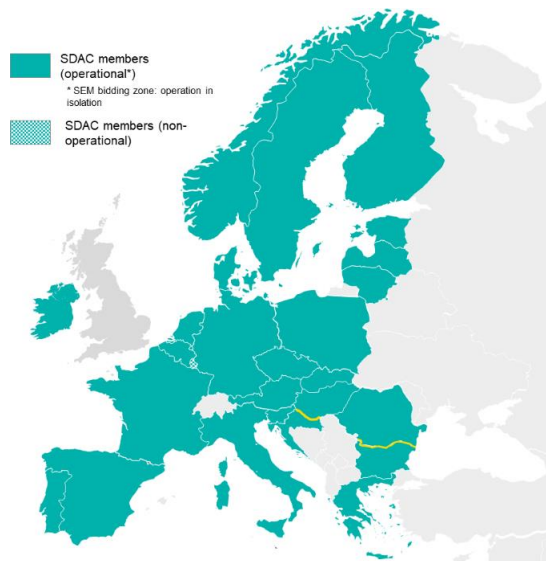
Figure 2.5. Countries participating in SDAC of EU wholesale electricity market [59]

A day-ahead market simulation tool called "Simulation facility" (SF) is available to many European TSOs. SF has the access to all European historical day-ahead market data and uses the same algorithm as the SDAC – the Euphemia – to run day-ahead market simulations. The

detailed description and methods of the Euphemia are given by [30] and is consistent with theory given in the Chapter 1.4. SF gives its users a possibility to run simulations with historical or updated (user-defined) data or their combination and to get an updated market results from such simulations.

For the purpose of this simulation a collaboration with the Latvian TSO AS Augstsprieguma Tīkls (AST) was initiated, and AST conducted a simulation in the SF using the historical power market data for the year 2020. The year 2020 was chosen as the most recent full year on the moment of conducting the simulation. It was also decided for the sake of SEW calculation to only simulate the day-ahead market and not the intraday market as the day-ahead power market is the largest power market (by volume of traded electrical energy) – e.g., according to historical market data available in Nord Pool AS power exchange [60]. In the opposite, the energy volume traded in the intraday power market in the Baltic Countries, the region of interest for this simulation, usually forms only a few percent of the energy volume traded at the day-ahead market. Due to this the day-ahead market is the one mostly impacted by potential cross-zonal capacities' reduction and the day-ahead market is the one having a major effect on the power price.

- Simulation set with forecasted data for 2030, 2040 and 2050

As the SF does only provide historic power market data and our task is to assess the SEW of LS scheme potentially to be installed in the nearest future, another alternative way of assessing the SEW for future scenarios has to be found. For this purpose an existing market simulation environment recently created by the researchers of the Riga Technical University was utilized.

Introduction

This market simulation environment was developed specially for the case of the Baltic power system, it is based on three synthesized mathematical models in Matlab2020b software used to simulate the Baltic power system and its market and to calculate the SEW. The three mathematical models of the Baltic Power System (BPS) and its market are: **Baltic Power System Basic (BPS_B)** [61] [62] [63], **Baltic Power System Market Simplified (BPS_MS)** model and **Baltic Power System Market Detailed (BPS_MD)** [63] model. Each of the mathematical models of BPS stands as a nested structure and consists of several sub models. In turn, mathematical sub models, or models of specific power plants, are realized by several specialized programming methods:

- Linear optimization [64]
- Mixed-integer linear optimization [65]
- Nonlinear optimization [65]
- Nonlinear autoregressive neural network with external prediction [66]
- Fourier transform [67] [68]

Brief description of the BPS_B mathematical model

The mathematical model of Baltic Power System Basic (BPS_B) consists of several connected mathematical models reflected in the Figure 2.6, all developed in-house by the RTU

Power Engineering faculty. The BPS_B model serves itself only as a topology basis for the market models BPS_MS and BPS_MD utilized in this simulation test case set. In trivial representation the BPS_B stands as one node power system and includes:

- Pumped-storage hydro power plants (PSHPP) [69] [70]
- Combined heat and power plants (CHP) [71] [72] [73]
- Hydro power plants (HPP) [74] [75] [76]
- Solar power plants (SPP) [77] [78]
- Wind power plants (WPP)
- Biomass power plants (BPP)
- Small hydro power plants (sHPP)
- Electric vehicles (EV) [77] [79] [80]
- Most expensive power plants (MEPP) (power plants with the highest marginal costs)
- Power demand [62]
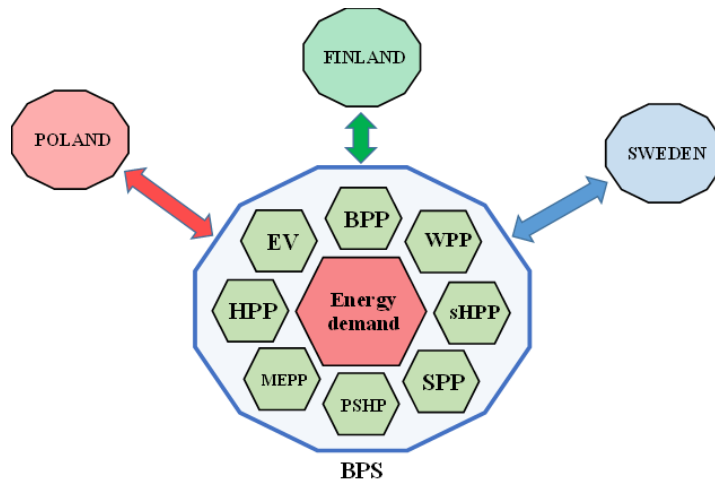
Figure 2.6. A diagram of the Baltic Power System Basic mathematical model [61]

Fundamental difference of applied BPS_MS and BPS_MD mathematical models

The models BPS_MS and BPS_MD are the mathematical models of the power market itself – on the top of the power system topology model BPS_B. The two created market models possess some fundamental differences which are presented in the Figure 2.7. The presence of speculative opportunity is the main difference between the two developed models.
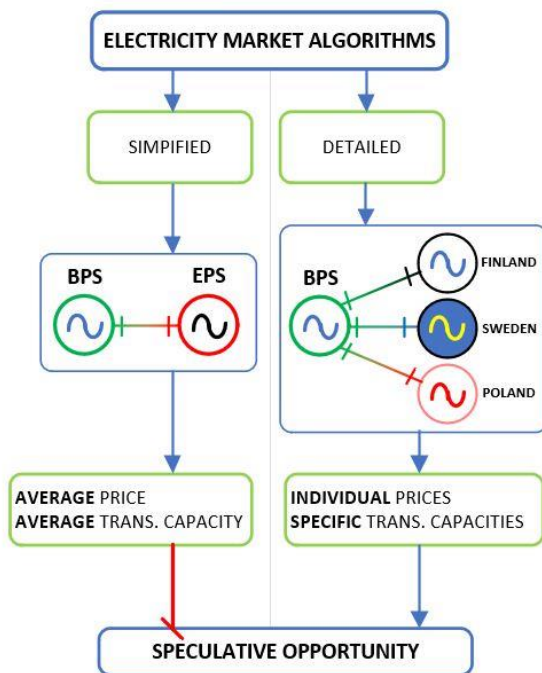
Figure 2.7. Fundamental difference of two applied mathematical market models of BPS.

In the 'Simplified' mathematical model of Baltic power market several fundamental assumptions are applied:

- Baltic Power System is connected to generation units of any external Energy Power System (EPS) via a virtual transmission line, which possesses a sum of all existing transmission line capacities, namely Estonia ↔ Finland transmission line capacity, Lithuania ↔ Sweden (SE4) transmission line capacity, Lithuania ↔ Poland transmission line capacity.

- Electricity price in the external Energy Power System stands as average value of the specific power systems` electricity prices i.e.

$$PriceEPS = AVERAGE(PriceFI, PriceSE4, PricePL) \qquad (2.4)$$

- At a specific time moment (in this research the discretization step equals to one hour) mutually exclusive action is possible i.e. power export from the BPS or power import into the BPS.

- The structure of BPS_MS is based on the application of Monte Carlo method for power import or power export issues

The 'Detailed' mathematical model of Baltic power system is closer to the real practical electricity market rules and to some extent approaches the Euphemia algorithm used in the simulation with historical data and described earlier in the thesis (chapter 1.4).

As seen in the Figure 2.7 the BPS is in this 'Detailed' model now connected to the corresponding external power systems via several specific transmission lines, with their own capacities. As result the BPS_MD mathematical market model has three individual connections with neighbour power systems, namely with Finland, Sweden and Poland. An important fact is that electricity prices in each of these power systems vary. These prices varying from system to system now may give an opportunity for power import and power export in/from the BPS simultaneously. As a result – a speculative opportunity arises. For instance, if the cheapest electricity price is in Finland power system, BPS can buy more power than for its own needs for trading power surplus to the power system with higher energy price. In that way BPS trades power with an objective to maximize self-profit. Not so different from the way Euphemia behaves.

Merit-order principle and generation/demand properties used in the simulation set

While the Euphemia uses a full merit-order with all the possible generation types present, the market models in this simulation set use a simplified merit-order presented in Figure 2.8. The generation types present in the merit-order for Baltic power market models BPS_MS and BPS_MD are:

- the renewable energy sources (RES) such as wind and sun set with marginal price of 10 EUR/MWh
- in the BPS_MS the import sources get average power price based on the price forecasts for all the import areas in the model
- in the BPS_MD the import sources get individual forecasted power prices for each individual import area in the model
- so called most expensive power plants (MEPP) with marginal price of either 120 or 240 EUR/MWh (low/high) depending on the scenario used for the simulation.
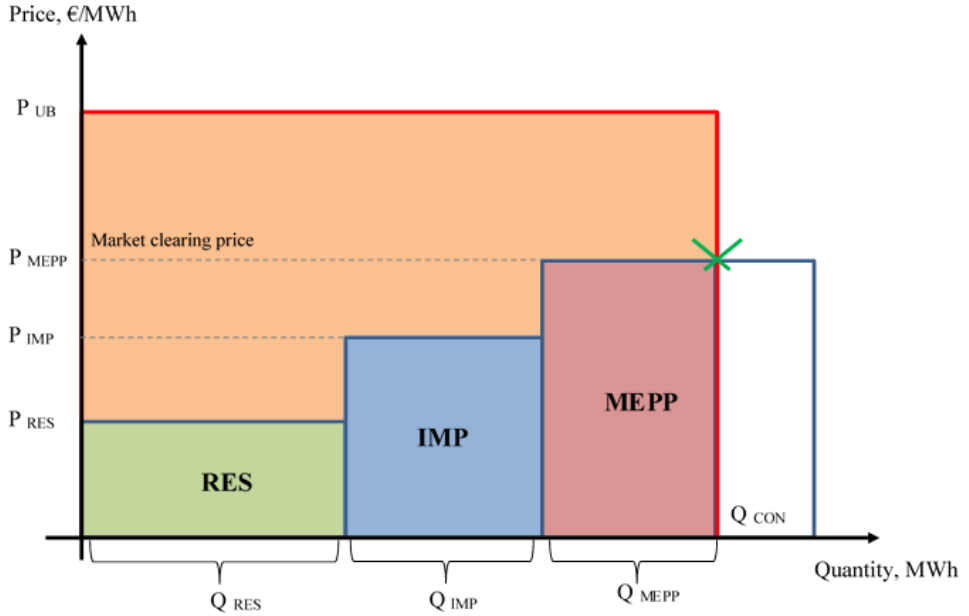
Figure 2.8. Merit-order of the market models utilized for the simulation set

The price forecasts for import areas are based on the historical power price data for the year 2019 [81] [82] [83] and on the forecast methods given by [67]. The forecasts were achieved the same way price forecasts in [62] were simulated. These can be found in the Annex I.

The forecasts for RES production volumes were based on the statistics of meteorological data from [84].

The forecast of the long-term available capacity forecast of the MEPP in the Baltic region was based on the [85] [86] [87] [88] [89] [90].

The demand model of the power system is simplified to represent a fully inelastic power demand given by its rectangular shape in the Figure 2.8. It is not an ideal representation but a simplified one, but still it gives an acceptable approximation to the real power demand curves observed in the Baltics during the winter season [14]. The price ceiling of the demand curve is 4000 EUR/MWh as given by the real power market in the Baltics [91].

With all this information available, the method from [67] was used to achieve reference price forecast for all of the scenarios of the upcoming simulation, similarly as this was done in the [62]. The simulation reference price forecasts are partially taken from [62] and partially recreated using the same price simulation technique and tools [62] utilized. The reference price forecasts for the simulation done in this thesis can found in the Annex II.

When it comes to the surpluses needed to calculate the SEW as stated by the Chapter 1.4, the producer surplus for these market models will then be:

$$Surplus_{PROD} = P_{MEPP} * Q_{CON} - (P_{RES} * Q_{RES} + P_{IMP} * Q_{IMP} + P_{MEPP} * Q_{MEPP}) \quad (2.5)$$

The consumer surplus is:

$$Surplus_{CON} = P_{UB} * Q_{CON} - P_{MEPP} * Q_{CON} \qquad (2.6)$$

And the SEW of the market is then as given by the theory in the Chapter 1.4:

$$SW = Surplus_{PROD} + Surplus_{CON} \qquad (2.7)$$

2.4.4. Practical usage of the calculated socio-economic welfare reduction and the congestion income

Changes in the socioeconomic welfare of the wholesale electricity market in different scenarios are evaluated as the total change of consumers' and producers' surpluses between the actual scenarios, also known as "the total surplus approach" as defined by the ENTSO-E guidelines [28]. But it shall be noted that the difference of socioeconomic welfare between scenarios shall not be accounted for during the whole year, but only during periods when Baltic Countries operate in the island mode. Therefore, the reduction of socioeconomic welfare of the market between the scenarios shall be calculated using following eq. (2.8):

$$SWR_M = \frac{SW_{Y_{Sx}} - SW_{Y_{Sy}}}{8760} * T_{isl\_mode} \qquad (2.8)$$

Where

SWR_M – reduction of socioeconomic welfare of the market, [Eur];

SW_{Y_Sx} – socioeconomic welfare of the market (consisting of producers' and consumers' surpluses) for the whole year Y in scenario "x"; [Eur];

SW_{Y_Sy} – socioeconomic welfare of the market (consisting of producers' and consumers' surpluses) for the whole year Y in scenario "y"; [Eur];

T_{isl_mode} – total average duration of island mode operation during a year, [h];

8760 – number of hours during a year, [h].

Total average duration of island mode operation during a single year is being calculated using following eq. (2.9):

$$T_{isl\_mode} = \omega * l * t \qquad (2.9)$$

Where

ω – number of outages of the synchronous link, [outages per 100 km per year];

l – length of the synchronous link, [km/100];

t – average duration of an outage of a synchronous link, [h].

Moreover, taking into account the fact that the day-ahead market cross-zonal capacities are provided by the TSOs to the market only once a day and not later than till 09:30CET on the day before the delivery day, there will always be a period for which the electricity market will not suffer from socioeconomic welfare loss – due to the fact that the changes of the cross-border

capacities are not instantly enforced but are only provided once a day and these values are locked firm for the day-ahead timeframe. The length of this period of no welfare loss for our case will depend on when exactly during the day the synchronous link between the Baltics and the CE trips and thus when the island mode operation occurs. TSOs have a deadline to deliver cross-zonal capacities for the day-ahead market not later than 9:30CET. If the island mode occurs right before 9:30CET and the TSO is still able to update the capacities for the day-ahead market, the results of day-ahead market for existing day will not change but the results for the next day will be affected giving a minimum of 14,5 hours (amount of hours between 9:30CET and 24:00 CET) of no effect onto the socioeconomic welfare loss. On the other hand if the island mode occurs right after 9:30CET and the TSO is not able to update the capacities for the day-ahead market, one will have a maximum of 24+14.5=38.5 hours of no effect onto the socioeconomic welfare loss. Authors of the paper are aware of that the TSOs would still be able to reduce intraday market capacities for existing and upcoming day but this possibility is neglected during the analysis presented in the paper due to relatively small trading volume at the intraday market. This means now that the reduction of the SEW has to be first calculated per outage case and then converted into an annual value. To take aforementioned into account, SWR_M shall be calculated according to an altered combination of following eq. (2.8) and (2.9), in which duration of a single outage of a synchronous link t is now used and reduced by an average value of (14.5+38.5)/2=26.5 hours (26.5 hours is the average time period during which there is no socioeconomic welfare loss for day ahead market) and then converted to an annual value by means of ω and l:

$$SWR_M = \frac{SW_{Y_{Sx}} - SW_{Y_{Sy}}}{8760} * \omega * l * (t - 26.5) \qquad (2.10)$$

It shall be noted, that in case if duration of an outage of a synchronous link t is less than 26.5 hours, there will be no socioeconomic welfare loss in day-ahead market.

During the first hours of island mode operation, when the TSOs have no possibility to reduce the cross-zonal capacities for the day-ahead market, so emergency power reserves would have to be activated in order to compensate for the reduction of the flows on the cross-border links with the amount specified for market simulation scenarios. Activation of such reserves would result in additional operational costs for the TSOs and therefore increase grid fees/tariffs. Therefore, the costs of reserve activation are assumed to be an additional to the socioeconomic welfare loss. Socioeconomic welfare loss due to the costs of reserves converted into an annual value by means of ω and l is calculated according to the following eq. (2.11):

$$SWR_R = 26.5 * FC_R * P_R * \omega * l \qquad (2.11)$$

Where
SWR_R – the total annual reduction of socioeconomic welfare from reserves activation, [Eur];
26.5 – average time period during which there is no socioeconomic welfare loss for the day-ahead market, [h];

FC_R – required (average) market power flow reduction on the HVDC interconnectors to reach the required grid stability criteria from the Chapter 2.3 [MW]. The number is calculated using the data from Chapters 1.5 and 2.3;

P_R – price of reserves' activation. [Eur/MWh].

The needed average market flow reduction FC_R is calculated as the average sum of results for all hours for all borders on the basis of simulation data. For each of the borders for each simulation scenario the initial market flow on the border is compared to the reduced capacity value. In case if the initial market flow on the border is higher that reduced capacity value, then the difference between these shows a need for reduction of flow on the specific border and is taken into account. In case if the initial market flow on the cross-border is lower than reduced capacity value, no reduction of market flow is needed for the border in the specific hour.

The price of reserves' activation (P_R) is assumed to be equal to the average value of the max prices of the manual frequency restoration reserves (mFRR) in the Baltic countries in 2020 added a small profit margin, summing up to 111 EUR/MWh.

Besides the socioeconomic welfare loss, as well as the expenses related to activations of the reserves, there is one more additional component to be taken into account – the congestion income of the TSOs. Congestion income appears in cases when capacities between bidding zones are not capable of transmitting all the required power flow to equalize prices between two adjacent bidding zones. In such situations one bidding zone has higher price than the other zone. Congestion income appears due to the fact that electricity seller in bidding zone A (with lower electricity price) receives smaller amount of money for the sold energy to the bidding zone B (with higher electricity price) than buyer in bidding zone B pays for the bought (imported) energy. Power exchange collects congestion income and distribute it among involved TSOs according to the local congestion income distribution rules. Congestion income in the Baltic region is being split between TSOs equally. As the congestion income can be used to reduce TSO grid fees it shall be taken into account as factor increasing socioeconomic welfare.

In a general case the congestion income for specific bidding zone border is being calculated in a following way:

$$CI_{A-B} = \sum_{h=1}^{n} MF_{A-B\_h} * APD_{A-B\_h} \qquad (2.12)$$

Where

CI_{A-B} – congestion income for bidding zone border between bidding zones A and B, [Eur/h];

h – hour number;

n – total number of hours of the analyzed period;

MF_{A-B_h} – market flow between bidding zones A and B at hour h, [MW];

APD_{A-B_h} – areas' A and B price difference at hour h, [Eur/MWh].

For the calculations regarding the congestion incomes relevant for the Baltic power system, five borders must be taken into account using the eq. (2.13) below. As the analysis of the

economic gain of the proposed LS scheme is performed for Baltic countries only, the calculations of congestion income must take into account only a half of the income from HVDC borders into the Baltics (the other half belongs to the TSOs on the other side of the HVDCs).

$$CI = \sum_{h=1}^{8760} 0.5CI_{FI-EE_h} + CI_{EE-LV_h} + CI_{LV-LT_h} + 0.5CI_{LT-PL_h} + 0.5CI_{LT-SE4_h} \quad (2.13)$$

Where

CI_{FI-EE_h} – congestion income for bidding zone border Finland-Estonia, [Eur/h];
CI_{EE-LV_h} – congestion income for bidding zone border Estonia-Latvia, [Eur/h];
CI_{LV-LT_h} – congestion income for bidding zone border Latvia-Lithuania, [Eur/h];
CI_{LT-PL_h} – congestion income for bidding zone border Lithuania-Poland, [Eur/h];
CI_{LT-SE4_h} – congestion income for bidding zone border Lithuania-SE4 (Sweden), [Eur/h].

2.4.5. VOLL estimations and data

The proposed LS scheme foresees LS activation to mitigate blackout and to replace the need to limit the cross-border capacities into the wholesale electricity market of the Baltics. Since the proposed LS scheme projects a negative monetary effect on the consumers, it shall also be evaluated and taken into account when evaluating economical effect of proposed LS solution. To evaluate the economic effect of the consumer disconnection under the LS activation, the VOLL values, duration and frequency of disconnection must be known.

A good overview of VOLL values is given in [26]. The VOLL values in [26] are given per consumer category type – household consumption, industry, services, etc. categories. In order to apply correct VOLL values, electricity consumption distribution in Baltic countries shall be known. In our study we have divided consumption into four parts: a) households; b) industry; c) transport; d) services and agriculture. Aforementioned consumption classification is based on data classification provided by European Environment Agency in [92]. The volume of VOLL for this study is calculated as an average VOLL value for the disconnected load volume due to LS in Baltic countries according to consumption sectors' proportion in total consumption.

It is important to notice, that LS appears only in some rare cases – when appearance of major incidents (outage of Baltic countries' HVDC links) happens exactly during the island mode operation. This is due to the fact that any major incident happening during the synchronous operation of Baltic countries with CE power system would not result in any emergency situation. Therefore to estimate negative effect of LS on customers we shall to evaluate not only VOLL and consumption pattern in Baltic countries, but also possibility of coincidence of the island mode of operation and major outage incidents. To estimate this, we need outage data for all of the current Baltic HVDC connections (LitPol Link, NordBalt, Estlink 2) – their outage numbers/outage frequency.

The effect of LS (load disconnection) in monetary terms shall be calculated in following way:

$$LSC = (\omega_{Estlink2} + \omega_{NordBalt} + \omega_{LitPolLink}) * \frac{T_{isl\_mode}}{8760} * P_{l\_disc} * t_{ls} * VOLL \quad (2.14)$$

Where

LSC – load shedding costs per year;

$\omega_{Estlink2}$ – average annual number of Estlink2 link outages, [outages];

$\omega_{NordBalt}$ – average annual number of NordBalt outages, [outages];

$\omega_{LitPolLink}$ – average annual number of LitPol link outages, [outages];

P_{l_disc} – disconnected load, [kW per outage];

t_{ls} – time of disconnection for shedded load, [h]

$VOLL$ – value of lost load, [Eur/kWh].

The disconnected load value (P_{l_disc}) is changing depending on scenarios under study in [10], where four scenarios with load disconnection have been analysed and there have been disconnected load (P_{l_disc}) with power of 200, 425.5 and 703 MW. For all the scenarios, for VOLL calculations, it is assumed that time of disconnection for shedded load (t_{ls}) is half an hour (30 minutes) – which allows emergency power reserves to restore normal state in power system and allow disconnected load to be connected to the network again.

It is important to note that the eq. (2.14) calculates costs of the load shedding based on the statistical average values of the outage rates of the Baltic HVDC connections and the statistical average outage rate of the synchronous link. That means that this eq. says that outage rate of an HVDC is evenly distributed through the whole year as is the outage rate of the synchronous link. In reality no one knows whether a major outage of an HVDC would happen exactly during the outage of the synchronous link or not – the probability for such kind of N-2 event is extremely hard to determine. This means also that in reality the cost of LS may also be zero as the event of major HVDC outage may happen outside the time when the synchronous link is out of operation. The eq. (2.14) provides the statistically average expected costs connected with the LS actions.

2.4.6. The concept of assessing the SEW gain of the proposed LS scheme

The total SEW loss due to the island mode operation without the proposed LS scheme, or said in another way – the total SEW gain given by the proposed LS scheme is given in the eq. (2.15):

$$SWR_{total} = SWR_M + SWR_R + CI \quad (2.15)$$

It has to be mentioned that another additional factors that theoretically may affect the economic feasibility of the proposed LS scheme, e.g. hardware and software procurement, installation, as well as operational expenditures, are believed to have a minimal fiscal impact and therefore not considered in this thesis.

For the operation of the proposed LS scheme 9 phase measurement units (PMU) are required as of the concept of the monitoring of the SC indicates [12]. According to [93] total installation costs of 9 PMUs may be in the range of 0.5-1.6 million USD. As the most major

high-voltage substations of the Baltic TSOs already possess basic communication infrastructure the costs for communication infrastructure for the PMUs are assumed to be negligible. Additionally, some negligible labour costs for the system logic installation, testing and calibration may arise. The operational costs of the system are assumed to be near-zero [14].

The mentioned capital costs of the proposed LS scheme are one-time costs which do not affect the operational costs. As these are capital costs and, as the chapters 3 and 4 will show, as these are almost negligible in comparison to the total gain in social welfare over e.g. 10 year period we do not take account of these capital costs in our assessment of the economic feasibility. Therefore, assuming the approach used in this thesis, the proposed LS scheme would be economically feasible in case if the following eq. (2.16) is fulfilled:

$$SWR_{total} > LSC \qquad\qquad (2.16)$$

3. MODELLING OF THE POWER SYSTEM WITH THE PROPOSED NOVEL LOAD SHEDDING SCHEME

In order to perform an assessment of the SEW gain of the proposed novel LS scheme two sets of power grid dynamic simulation case studies will be executed based on two different Baltic power grid models derived from models found in [44] and presenting a range of scenarios for the Baltic power system: from today's situation with little non-synchronous renewable generation of considerable size to a scenario with non-synchronous renewable generation supplying a major part of the electricity demand. Two different and independent sets of test cases on two different models depicting the Baltic power system in different simulation environments – Siemens PSSE ver. 34 and ETAP ver. 12.5 [94] [95] – are executed in order to cross-check the performance of our proposed LS concept and to prove its efficiency to keep the frequency within the operational limits of the power grid.

In addition, the test case presented in the chapter 3.1 will be compared to a real-life incident in the Baltic power grid with similar incident characteristics to the actual simulated test case.

3.1. Test Case Set No. 1

The first case study set will be simulated in Siemens PSSE ver. 34 software [94] taking a as a model of the Baltic power grid in island mode presented in [44] and enhanced with adding a set of synchronous condensers (SC): 3 SCs rated ca. 305 MVA each added to the busbar of every Baltic country – totaling 9 SC. The SC are of turbogenerator-type with active power set to 0, each having an inertia constant of H = 6.23 s, providing a total inertia of 17101 MWs. The other dynamic characteristics of the SCs for the model are provided by [14]. Additionally, three tie lines between Latvian and Lithuanian zones are now present to depict the realities of the Baltic power system The rest of model characteristics are identical to that in [44]. A diagram of the modelled grid can be seen in Figure 3.1. An overview of the system parameters in the different modelled scenarios is seen in Table 3.1

Figure 3.1. Schematic diagram of the modelled Baltic power grid for test case set No. 1.

Table 3.1. Grid model parameters for different modelled scenarios, test case set No.1, MW/MWs in italic.

	Scenario			
	A	B	C	D
Total generation before disruption	2567	2548	2623	2686
-of it renewable non-synchronous	100	700	1500	2500
Total load	3700	3700	3700	3700
Total import	1700	1700	1600	1530
Total export	500	500	500	500
Total post-contingency system inertia H_{tot_post}	*29,779*	*36,739*	*24,768*	*18,091*
Gen. loss event	TEC2, 800 MW	HVDC, 700 MW	HVDC, 700 MW	HVDC, 700 MW

For all the scenarios of the test case set No.1 the most severe disturbance available will be modelled: tripping of TEC2 with 800 MW or HVDC import cable with 700 MW. Scenario A depicts a situation with almost no renewable generation feeding into the power system. Scenarios B, C and D have increasing renewable power generation levels displacing the generation on the top of the merit-order, which for the Baltics is TEC2. This means the tripping of TEC2 with full power is not possible in the scenarios B, C and D and therefore the tripping of the 700 MW HVDC cable becomes the largest incident. Active power injections of the SC on each country busbar will then be examined and used to draw the basics of the proposed LS concept. The total SC active power injections ΔP_{SC} will be monitored from $t \geq 20$ ms from the start of contingency, as 20 ms is one swing period for a 50 Hz AC grid and measurement accuracy at Δt under 1 swing period can be problematic due to the function principles of the voltage and current measurement units, as well as due to the sub-transient and transient electromagnetic processes in the rotor-stator pair of any synchronous generator. This will be the procedure for measuring ΔP_{SC} for the test case set No. 2 in the chapter 3.2 as well. For all scenarios of the test case set No. 1 a separate simulation for cases with no LS, with conventional

UFLS and with the proposed novel LS method will be executed in order to compare the frequency responses. The parameters for the conventional UFLS for the test case set No. 1 are given by Table 3.2 with activation time delay of 0.17 s after threshold has been reached. One can also see that the parameters in the Table 3.2 do not include the special UFLS stage as given by the Table 1.1: according to [14] this special stage is not operated in normal operating conditions.

Table 3.2. Conventional UFLS parameters, test case set No. 1.

	Load Shedding Step Number, n					
	1	2	3	4	5	6
Freq. threshold, Hz	48.8	48.6	48.4	48.2	48.0	47.8
$P_{load\_UFLS\_n}$, %	5.4	6.1	7.5	6.4	5.4	4.4

Note that the triggering of load shedding using the measured SC power injection value ΔP_{SC} can be realized in various ways. For the test case set No. 1 we present the results corresponding to a simple scheme of triggering the LS by the value of the ΔP_{SC} (another different scheme for the test case set No. 2 will be described in the Chapter 3.2): if a power injection ΔP_{SC} is detected and measured, then the load is disconnected according to the following algorithm:

IF $\Delta P_{SC} > P_{load\_UFLS\_1}$ AND IF $\Delta P_{SC} < (P_{load\_UFLS\_1} + P_{load\_UFLS\_2})$ then $P_{load\_novel\_LS} = P_{load\_UFLS\_1}$;

IF $\Delta P_{SC} > (P_{load\_UFLS\_1} + P_{load\_UFLS\_2})$ AND IF $\Delta P_{SC} < (P_{load\_UFLS\_1} + P_{load\_UFLS\_2} + P_{load\_UFLS\_3})$ then $P_{load\_novel\_LS} = P_{load\_UFLS\_2}$;

…

where $P_{load\_UFLS\_1}$, $P_{load\_UFLS\_2}$, … are loads shed carried out by the corresponding step of conventional UFLS (see Table 3.2). $P_{load\_novel\_LS}$ is load shed cared out by the proposed LS method. The total load shed by conventional UFLS is the sum of all the relevant steps $P_{load\_UFLS} = P_{load\_UFLS\_1} + P_{load\_UFLS\_2} + …$

For each scenario, the volume of load shed by the conventional LS method and novel proposed method is the same. This means that first a simulation with the existing UFLS scheme was executed and the volume of load shed noted. Then for the same scenario – a simulation with the novel LS scheme was executed implementing the LS volume equal to the one from the simulation with the existing UFLS scheme. Observance of this volume equality makes it easier to compare the efficiency of both compared LS schemes. The LS done with the proposed novel scheme is activated with time delay of no more than 0.4 s after the triggering of the scheme (approximately 0.5 s after the disturbance itself).

3.1.1. Scenario A

An outage of TEC2 synchronous generation of 800 MW is simulated at t = 5 s and the LS activated according to the proposed novel LS method. The active power response of SCs can be seen in Figure 3.2: the SCs in all three countries react instantly with the SC closest to outage

location injecting more active power; at t ≈ 5.5 s the drop of active power injections due to LS activation can be seen. Active power responses are scaled p.u. to the base MVA rating of 1200 MW. Figure 3.3 shows the frequency responses of all simulations within scenario A, frequency is scaled p.u. to the base of 50 Hz.
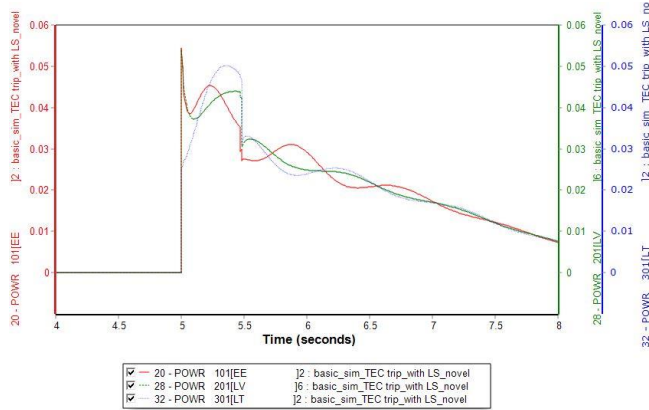
Figure 3.2. Active power injections of the SC, scenario A with novel LS method.
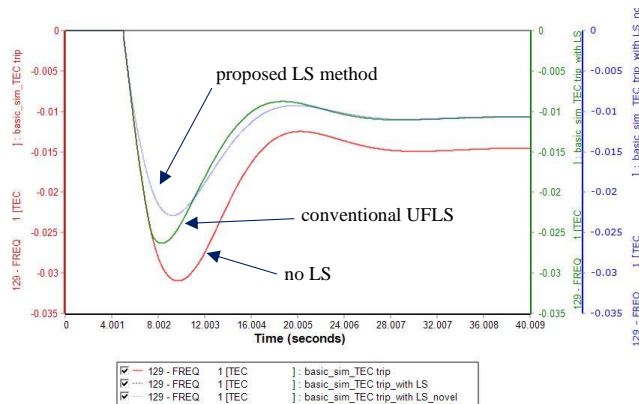
Figure 3.3. Frequency responses, scenario A.

In the Figure 3.2 the instantaneous active power response of Estonian and Latvian SCs (red and green curves) being closest to the tripped generator reaches 54 MW each, the response of the Lithuanian SC (blue curve) is around 32 MW and it reacts on the disturbance much slower as being furthermost from the tripped generator in the model. The ΔP_{SC} = 420 MW. Figure 3.3 shows that with conventional UFLS frequency falls to 48.7 Hz and with proposed LS method – to 48.85 Hz.

3.1.2. Scenario B

An outage of HVDC import cable of 700 MW is simulated at t = 5 s and no conventional UFLS is activated due to insufficient fall in frequency. In the same way a simulation with the

proposed LS method is conducted. The active power response of SCs can be seen in Figure 3.4: the SCs in all three countries react instantly with the SCs closest to outage location injecting more active power. Active power responses are scaled p.u. to the base MVA rating of 1200 MW. Figure 3.5 shows the frequency responses of both simulations within scenario B, frequency is scaled p.u. to the base of 50 Hz.
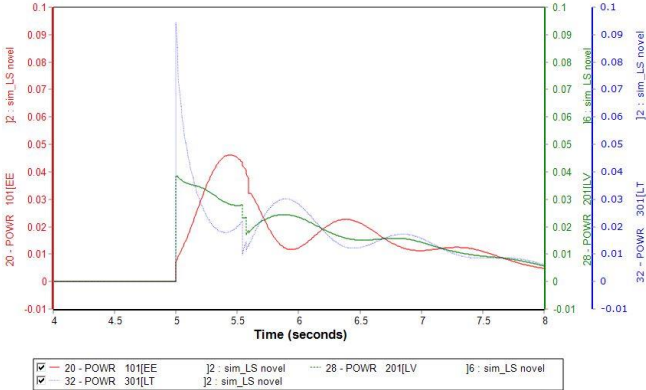
Figure 3.4. Active power injections of the SC, scenario B with novel LS method.
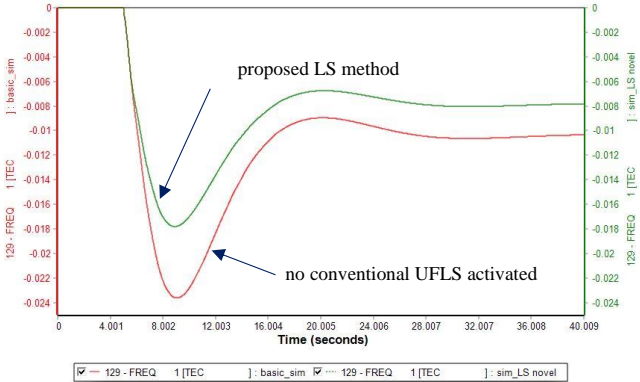
Figure 3.5. Frequency responses, scenario B.

In the Figure 3.4 the instantaneous active power response of Estonian and Latvian SC (red and green curves) are 11 MW and 46 MW, the response of the Lithuanian SC (blue curve) being closest to the tripped HVDC cable is around 89 MW. Estonian SC reacts on the disturbance much slower as being furthermost from the tripped HVDC cable in the model. The ΔP_{SC} = 438 MW. Figure 3.5 shows that the frequency falls to 48.81 Hz und is not sufficient to activate the conventional UFLS; with the proposed LS method activated the frequency falls only to 49.1 Hz.

The scenario B stands out from the other scenarios in the test case set by both a large amount of system inertia and a large amount of available spinning reserves, that also explains the fact that in this scenario the classical UFLS is not activated—the primary regulators of the

synchronous generators limit the fall of the frequency. The scenario also shows a potential strength of the proposed LS method for high-inertia cases: it is activated and contributes to limit the fall in frequency also in cases when no conventional UFLS is expected to be activated.

3.1.3. Scenario C

An outage of HVDC import cable of 700 MW is simulated at $t = 5$ s and the LS activated according to the proposed method. The active power response of SCs can be seen in Figure 3.6: the SCs in all three countries react instantly with the SCs closest to outage location injecting more active power; at $t \approx 5.5$ s the drop of active power injections due to LS activation can be seen. Active power responses are scaled p.u. to the base MVA rating of 1200 MW. Figure 3.7 shows the frequency responses of all simulations within scenario C, frequency is scaled p.u. to the base of 50 Hz.
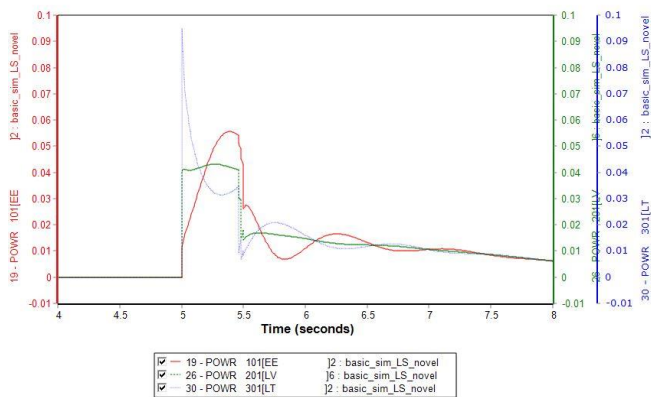
Figure 3.6. Active power injections of the SC, scenario C with novel LS method.
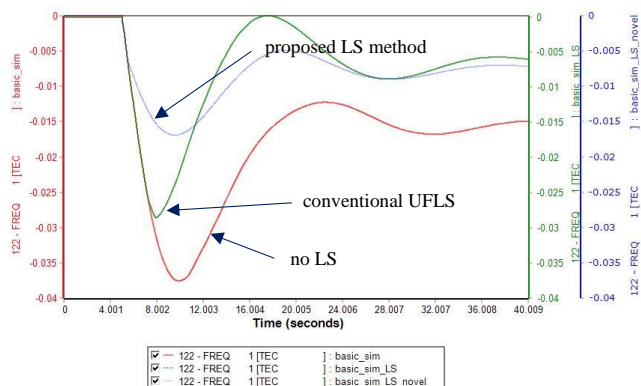
Figure 3.7. Frequency responses, scenario C.

In the Figure 3.6 the instantaneous active power response of Estonian and Latvian SC (red and green curves) are 18 MW and 49 MW each, the response of the Lithuanian SC (blue curve) being closest to the tripped HVDC cable is around 91 MW. Estonian SC reacts on the

disturbance much slower as being furthermost from the tripped HVDC cable in the model. ΔP_{SC} = 475 MW. Figure 3.7 shows that with conventional UFLS frequency falls to 48.6 Hz and with proposed LS method – to 49.15 Hz.

3.1.4. Scenario D

An outage of HVDC import cable of 700 MW is simulated at t = 5 s and the LS activated according to the proposed LS method. The active power response of SCs can be seen in Figure 3.8: the SCs in all three countries react instantly with the SC closest to outage location injecting more active power; at t ≈ 5.5 s the drop of active power injections due to LS activation can be seen. Active power responses are scaled p.u. to the base MVA rating of 1200 MW. Figure 3.9 shows the frequency responses of all simulations within scenario D, frequency is scaled p.u. to the base of 50 Hz.
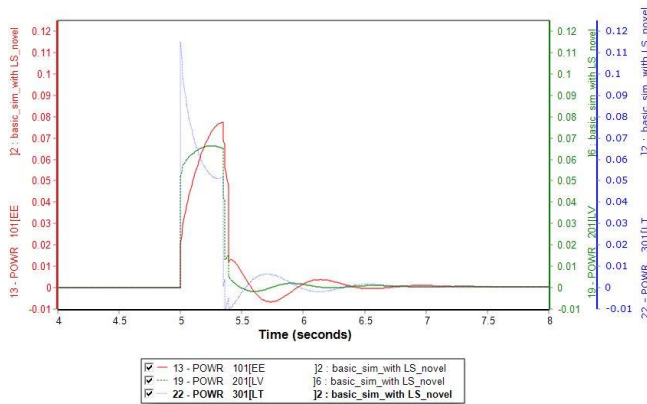
Figure 3.8. Active power injections of the SC, scenario D with novel LS method.
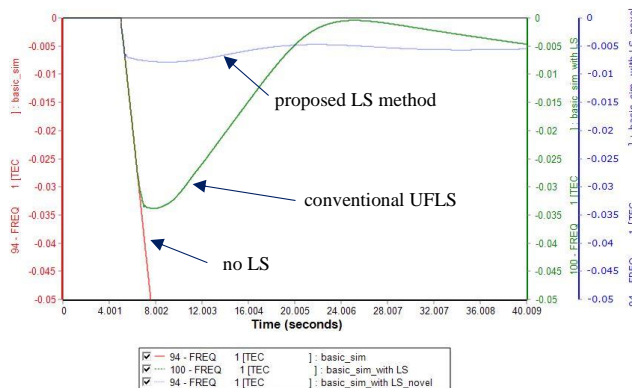
Figure 3.9. Frequency responses, scenario D.

In the Figure 3.8 the instantaneous active power response of Estonian and Latvian SCs (red and green curves) are 36 MW and 68 MW each, the response of the Lithuanian SC (blue curve) being closest to the tripped HVDC cable is around 118 MW. Estonian SC reacts on the

disturbance much slower as being furthermost from the tripped HVDC cable in the model. ΔP_{SC} = 666 MW. Figure 3.9 shows that with conventional UFLS frequency falls to 48.3 Hz and with proposed LS method – to 49.6 Hz.

The summary of results of test case set No. 1 can be seen in Table 3.3

Table 3.3. Result summary, test case set No. 1.

	Scenario			
	A	**B**	**C**	**D**
ΔP_{SC}, MW	420	438	475	666
P_{load_UFLS}, MW	200	0	425.5	703
P_{load_UFLS}, % of total load	5.4	0	11.5	19
$P_{load\_novel\_LS}$, MW	200	200	425.5	703
Frequency nadir when UFLS does not activate (scenario B), Hz	-	48.81	-	-
Frequency nadir conventional UFLS, Hz	48.7	-	48.6	48.3
Frequency nadir novel LS method, Hz	48.85	49.1	49.15	49.6

3.2. Test Case Set No. 2

The second test case study set is also based on another model previously presented in [44]. The model (depicted in Figure 3.10) has a more detailed depiction of Latvian power system but depicts Estonian and Lithuanian power systems as grid equivalents – thus providing a different dynamic response to disturbances than the model in the test case set No. 1. The total rated power of the grid equivalents are 990 MVA for EE and 400 MVA for LT. This model also has 3 SC present (SC1, SC4 and SC6) rated at 305 MVA in the Latvian power grid as in the model of the test case set No. 1. The largest traditional generation plants are cogeneration plant CHP2 and hydro power plant HPP. Some of the traditional generation sources were replaced with wind parks (WTG2, WTG4 and WTG6) in order to imitate the increasing penetration of the non-synchronous renewable sources in the future. Despite this presence of the renewable sources the share of synchronous generation in the total load of scenarios A and B of the test case set are 91% which is exceptionally high for the Baltic power system today. This means the scenarios A and B represent historic rather than future situation. Scenario C on the other hand gives a realistic image of today's situation with a portion of synchronous generation in the total load around 50%. An overview of the test case set scenario parameters in the different modelled scenarios is seen in Table 3.4.

Table 3.4. Grid element parameters for different modelled scenarios, test case set No. 2, MW/MWs in italic.

Scenario	CHP2	HPP	EE	LT	WTG2	WTG4	WTG6	WTG10	Gen. Loss Event	Total System Inertia
A	800	220	670	380	128	40	120	-	EE	*15,760*
B	-	800	990	400	128	40	120	-	HPP	*12,150*
C	800	-	50	350	128	40	120	640	CHP2	*12,148*
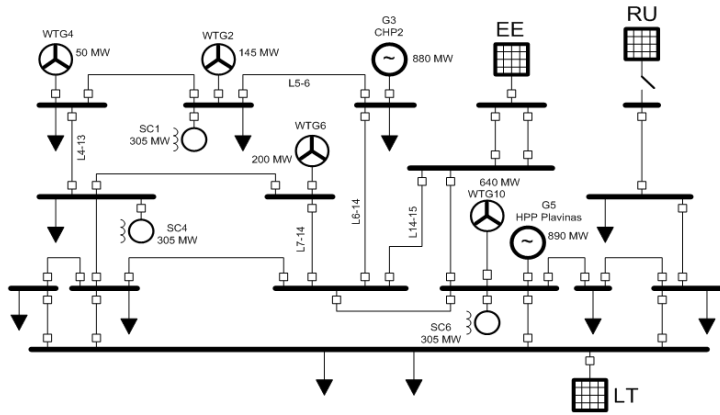
Figure 3.10. Schematic diagram of the modelled Baltic power grid for test case set No. 2.

Three scenarios (A-C) were simulated using ETAP 12.5 electrical software [95]. The goal of simulation was to explore the system frequency response under various loss-of-generation events. Total load of the Latvian grid is assumed to be ca. 2400 MW for all cases. Approximately half of the consumption is covered by in-house generation capacity with the remaining power imported from EE and LT. The loss-of-generation events were simulated by disconnecting one of the major generation source.

For the second set of tests, simulations were first done with conventional UFLS and then with the proposed LS method. Additionally, now we use a different scheme (compared to the one described in Section 3.1) for choosing the volume of the load to be disconnected. We assume that the volume of the load to be disconnected – $P_{load\_novel\_LS}$ is proportional to the injection power ΔP_{SC} of all SC according to eq. (3.1):

$$P_{load\_novel\_LS} = K * \Delta P_{SC} \tag{3.1}$$

where K is the gain coefficient for the LS scheme response. Ideally the coefficient K is to be predicted as close as possible to the coefficient K_r appearing in the eq. (2.2). The parameters of conventional UFLS are given by the Table 3.5 with activation time delay of 0.3 s after threshold has been reached. The total amount of load shed by the conventional UFLS is P_{load_UFLS}.

Table 3.5. Conventional UFLS parameters, test case set No. 2.

	Load Shedding Step Number, n					
	1	2	3	4	5	6
Freq. threshold, Hz	49.0	48.8	48.6	48.4	48.2	48.0
$P_{load\_UFLS\_n}$, %	5	5	10	10	10	10

The load shed with the novel LS method with time delay of 0.3 s after the disturbance. In cases where the amount of load shed by the novel LS method was not sufficient to limit the fall in frequency the conventional UFLS will kick in according to the thresholds in Table 3.5.

For each scenario of test case set No. 2 simulations with generation loss event at t = 0.5 s were carried out: with conventional UFLS and with novel LS method with coefficient K = 1; for scenario B also simulations with coefficients K = 2 and K = 3 were executed to reach the best frequency result within the criteria of added value of the novel LS method. For simulations with the novel LS method the conventional UFLS scheme was still active and it contributed with additional shed load as we see in the scenarios B and C. The simulation results for all scenarios of the test case set No. 2 are given in the Table 3.6. The frequency responses of the simulations of scenarios A and B are given in Figure 3.11 and Figure 3.12.

Table 3.6. Result summary, test case set No. 2.

Scenario	ΔP_{gen_loss}, MW	ΔP_{load_UFLS}, MW	Conventional UFLS f_{min}, Hz	ΔP_{SC}, MW	Novel Approach LS with K = 1 + Additional Load Shed by Conv. UFLS		Novel Approach LS with K=2 + Additional Load Shed by Conv. UFLS		Novel Approach LS with K=3 + Additional Load Shed by Conv. UFLS	
					f_{min}, Hz	Add. Conv. UFLS, MW	f_{min}, Hz	Add. Conv. UFLS, MW	f_{min}, Hz	Add. Conv. UFLS, MW
A	670	120	48.9	150	49.06	-	49.46	-	49.67	-
B	800	960	48.1	280	48.4	480	48.72	240	49.48	-
C	800	480	48.45	330	48.9	120	N/A	-	N/A	-
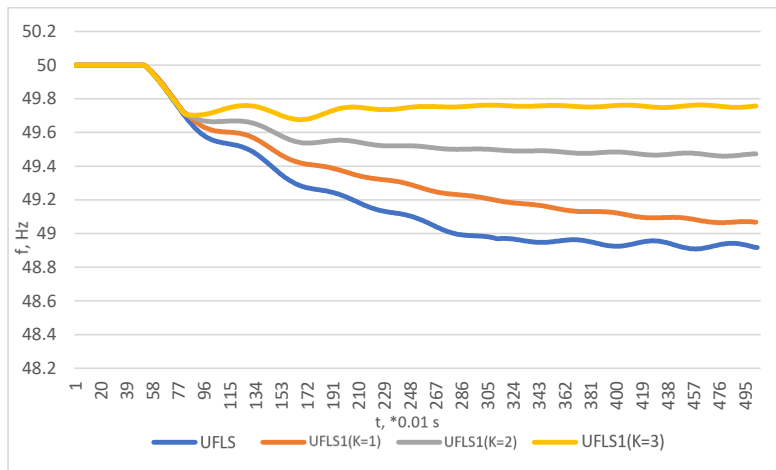
Figure 3.11. Frequency responses, scenario A.
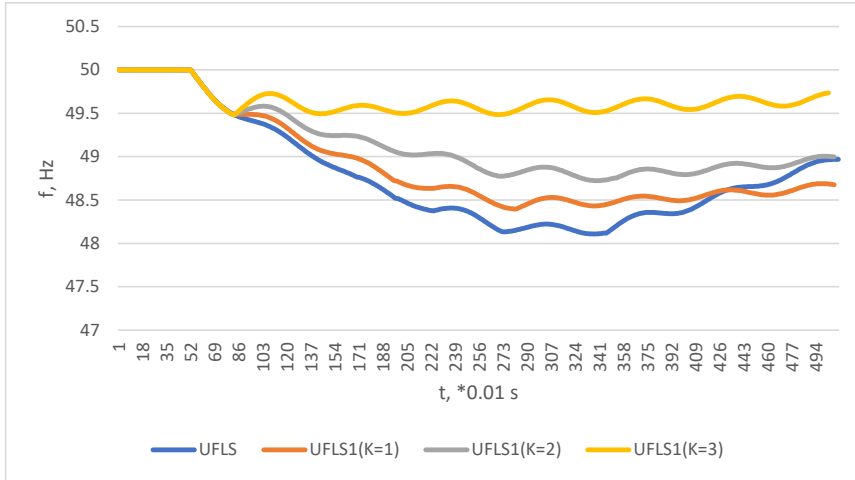
Figure 3.12. Frequency responses, scenario B.

The scenarios in the test case set No. 2 were very diverse in terms of level of total system inertia and the parameters of the primary frequency control regulators. Scenario A had a high system inertia, which explains the minimal amount of P_{load_UFLS} and ΔP_{SC}. In scenario B the system inertia was high but the power reserves of all of the remaining synchronous generators in the system were zero as the delivered active power of all remaining synchronous machines is equal to their rated apparent power: it is a rather unrealistic scenario but nevertheless included in the test case set. The amount load shed by conventional UFLS P_{load_UFLS} in scenario B was exceptionally large and even with this large amount of load shed the frequency falls down to unacceptable value of 48.1 Hz. This all due to the missing capability of the synchronous generators in the system to contribute with any active power. The response of the SC ΔP_{SC} in this scenario is also almost the double of that in scenario A with a similar level of system inertia. In the scenario B the coefficient K had to be brought up to K = 3 so that the $P_{load\_novel\_LS}$ could match the P_{load_UFLS} for that scenario and prevent the fall of frequency to an unacceptable level. The proposed LS method shows clearly its advantage in this particular scenario, but also highlights the fact that the novel approach LS coefficient K may have to possess a dynamic value proportional to the total system inertia. The determination of an algorithm for estimation of K for real system applications will be one of the topics of further research.

Scenarios C and D have also shown that the proposed LS method significantly improves frequency response, especially for the low-inertia scenario C.

3.3. Real life incident comparison with test case set no. 1

An incident was registered in the Baltic power grid on the morning of 09.06.2020 when Riga TEC2 delivering full power of 800 MW experienced an unplanned disconnection from the power grid. The outage of the power plant was unintentionally identical to the one simulated in the scenario A of the chapter 3.1, but here the Baltic power grid was working in the normal

synchronous mode with the UPS/IPS system and not in an island mode which is only expected to occur after the synchronization with ENTSO-E grid in 2025. Nevertheless, it is interesting shortly to analyse also this incident.

The network state before the incident have been weakened by a few scheduled and few unplanned outages:

- the NordBalt HVDC interconnector (700 MW) between Sweden and Lithuania was out of service due to an earlier failure. The power deficit was covered by the largest power plant Riga TEC2 which was operating at full power (800 MW);
- one of the two (at that time) TEC2 outgoing 330 kV transmission lines was disconnected because of the scheduled renovation works thus, leaving the TEC2 connected with the rest of the grid through a single 330kV underground cable and several 110 kV lines.

The contingency was triggered by a short circuit in the 330kV underground cable. Comparing with short circuits in overhead transmission lines, 330 kV cable short circuit is a rare event. The cable was disconnected by protection system in 80 ms after short circuit. The full power of TEC2 was redistributed on the 110 kV network. Because of the limited thermal capacity of the 110 kV grid, several transmission lines were overloaded and then disconnected by line protection devices. The lines disconnection took place randomly thus, the entire network was uncontrollably separated. Uncontrolled splitting resulted in 27 substations remaining without power infeed and large regions, including significant part of Riga, remained without power supply. TEC2 was shut down completely and power was sourced from the hydroelectric power stations (HPP) (Figure 3.13). According to incident aftermath, about 140000 customers were affected. The system restoration time was relatively short; system was fully restored within 2 hours. Such rapid recovery was partially facilitated by the availability of power reserve from hydroelectric power plants.

This incident shows a system degradation scenario with a N-2 state when the short circuit happens. Short circuit shifts the system to N-3 condition which then followed by cascading and uncontrolled splitting of the network.

The frequency response of the Baltic power grid in the mode of synchronous operation with UPS/IPS grid is shown in Figure 3.14. The incident of 09.06.2020 showed that an outage of fully loaded Riga TEC2 in the mode of synchronous operation with UPS/IPS grid does not affect the frequency in a major manner: the frequency nadir reached 49.942 Hz and the average frequency fall gradient of 0.01 Hz/s. These values do not breach requirements of the EU guidelines on electricity transmission system operation (SOGL) on frequency deviations [96].
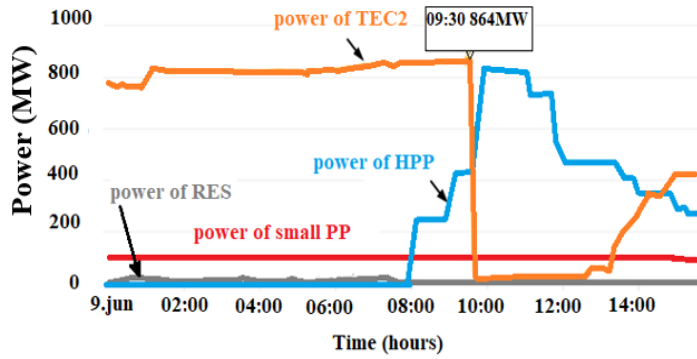
Figure 3.13. Power generation during the 09.06.2020 incident
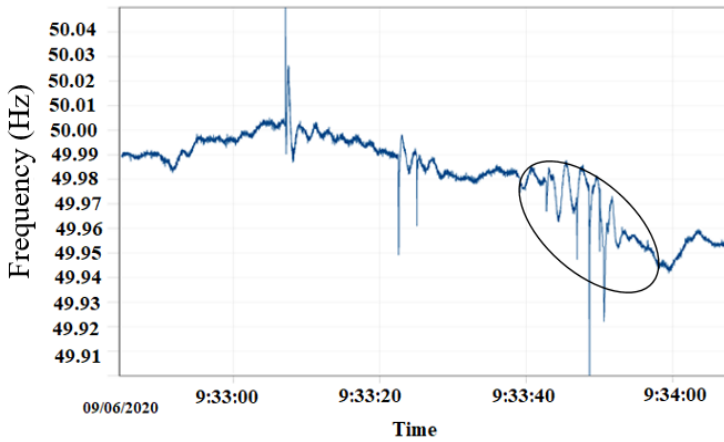
Figure 3.14. Frequency response of Baltic power grid during the 09.06.2020 incident.

4. SOCIO-ECONOMIC ASSESSMENT OF THE EFFECT OF THE PROPOSED NOVEL LOAD SHEDDING SCHEME. HISTORICAL INPUT DATA.

4.1. General info and definition of study case scenarios

The thesis will now move from technical questions of the proposed LS scheme and will address the economic impact. The thesis will assess the gain of socio-economic welfare of introducing the proposed novel LS scheme. A case study of the socioeconomic welfare gain brought by the proposed novel LS scheme will be executed with Baltic states as a study subject and by using the historical power system and power market data for 2020. The case study will assess the proposed LS scheme's contribution to lower the socio-economic costs of the islanding events of the Baltic power system.

For the purpose of the case study Latvian TSO AS "Augstsprieguma Tīkls" (AST) on the formal request of the author has performed simulations in the SF and formally provided results already in processed and combined form. Simulations have been performed using the actual historical data for the year 2020 for three scenarios described below:

1) Scenario Nr.1. The reference case. Using historical data on transmission capacities on all the borders except Latvia-Russia and Lithuania-Belarus borders, where 0 (zero) MW cross-zonal capacity has been used (these particular borders are not relevant for the post-2025 situation);

2) Scenario Nr.2. The maximum capacities of HVDC links of Finland-Estonia (only applicable to Estlink 2 capacity), Sweden-Lithuania and Poland-Lithuania borders have been reduced 50 MW below the nominal (maximum) capacity. In case if historical capacity on the border for exact simulation hour has been already below "nominal capacity", historical value has not been changed. 0 (zero) MW cross-zonal capacity has been used on Latvia-Russia and Lithuania-Belarus borders;

3) Scenario Nr.3. The maximum capacities of HVDC links of Finland-Estonia (only applicable to Estlink 2 capacity), Sweden-Lithuania and Poland-Lithuania borders have been reduced to the level of 400 MW. This scenario is the most realistic scenario for the post-2025 situation expected for the Baltic power system when operating in an island mode [14]. In case if historical capacity on the border for exact simulation hour has been already below 400 MW, historical value has not been changed. 0 (zero) MW cross-zonal capacity has been used on Latvia-Russia and Lithuania-Belarus borders. This scenario corresponds to the expected behavior of the Baltic TSOs during island mode of operation of the post-2025 situation described in the ch. 2.3.

The wholesale electricity market simulations have been made for the whole year 2020 with hourly resolution and the results of simulations coming from SF, among others, included consumers' surplus (in Euro), producers' surplus (in Euro), flows on bidding-zone borders (in MW), as well as electrical energy prices (in Euro) at each bidding zone. Consumers' and producers' surpluses formed socio-economic welfare of the wholesale electricity market itself,

but bidding-zone borders flows, in combination with electrical energy prices allowed to calculate so called "congestion income" volume, the nature and purpose of which is described further in the paper.

The case study uses the exact same load disconnection scenarios from [12] or observed in the Table 3.3 – 200MW, 425.5MW and 702MW of load disconnected by the proposed novel LS scheme, the loads are assumed disconnected for 0.5 h as this is a maximal time for reserve activation and a normalization of the situation following a major frequency disturbance [14]. The both market limitation scenarios – Scenario Nr.2 and Nr.3 are used as described in this subchapter. The simulation parameter and the resulting case study number overview is presented in the Table 4.1.

Table 4.1. SEW with historical data simulation parameter overview

Load disconnected /energy not served due to the LS scheme, MW/MWh	Scenario nr.	Case study Nr.
200/100	Scenario Nr.2.	1.A.
	Scenario Nr.3.	1.B.
425.5/212.75	Scenario Nr.2.	2.A.
	Scenario Nr.3.	2.B.
703/351.5	Scenario Nr.2.	3.A.
	Scenario Nr.3.	3.B.

It is worth mentioning that the LS scenarios from [12] were based on different amount of non-synchronous generation present in the Baltic power system. In that sense the current case studies ascending from 1 to 3 can be seen as case studies with increasing portion of non-synchronous electricity supply in the Baltic power system, regardless of the source of the supply (wind, solar, HVDC etc.) – with the case nr. 1 having the least amount of non-synchronous supply and case nr. 3 – the largest amount of non-synchronous supply. Increasing the amount of non-synchronous supply does results in decreasing power system inertia and in increasing amount of load needed to be shed in order to stabilize the frequency during a major incident.

4.2. Statistics of AC lines outages and major incidents for the study case

As mentioned in the chapter 2.4.2 a study based on the data from [51] [52] [53] [54] [55] [56] on AC line outage rate has been performed in order to gain outage rates and outage durations for the case study for this paper. An overview of that statistical data from the study are presented are in Table 4.2.

Table 4.2. Average outage rates and outage duration of single circuit AC lines

Voltage level, kV	Outage rate, times/100km/year	Outage duration, h
230kV	0,73	10,71
500kV	0,60	8,19
240kV	0,92	5,77
345kV	2,22	61,84
500kV	0,24	12,14
220kV	0,60	10
330kV	0,50	12
500kV	0,40	17
330kV	1,10	-
400kV	0,49	-
500kV	0,50	-
380-420kV	1,22	-
380-420kV	0,43	-

Average values of outage rates and outage durations from Table 4.2 will be used for this thesis, previously excluding the extreme small and large failure rate and outage duration in order to avoid the statistical extremas and to improve the overall quality of the results. Average outage rate for extra-high voltage lines per 100km of line per year is thus found to be 0.68 and the average outage time – 11.67 hours.

[54] provides also data on ratio between outages of single-circuit and double-circuit (common mode outage) AC lines. This source data shows that the ratio between single-circuit and double-circuit (common mode outage) AC line outage rates/outage frequencies is 0.2 and the ratio between single-circuit and double-circuit (common mode outage) AC line outage durations varies between 6.75 to 18 (in this study an average value of 12.38 is used).

This means, that using aforementioned data and ratios for conversion, for a double circuit line an average common-mode outage rate per 100km of line per year is 0.14 and an average outage time is thus 144 hours. These values can be transponded onto the data on LitPol link to get relevant outage rates and time for the synchronous connection between the Baltic and CE power systems. According to [49] and [50], length of the LitPol link part from Alytus substation in Lithuania to the Lithuania–Poland border is 48km, LitPol link part from the Lithuania–Poland border to the Elk substation in Poland is 106km and link part from Elk substation to Lomza substation in Poland is 84km – giving a total length of LitPol link of 238km. With the line length we can expect LitPol link to have a common-mode outage of both circuits $\omega * l = 0.324$ times per year and with duration of $t = 144$ hours. Thus giving T_{isl_mode} to be 46.66 hours.

Statistics on number of outages for Baltic HVDC links (LitPol link outage number statistics is used to represent the future HarmonyLink) has been taken from Nord Pool AS UMM system

[57] and represents assumed major incidents for this paper. Average outage number per year per HVDC connection is given in Table 4.3.

Table 4.3. Outage rates of HVDC links per year

HVDC link	Outages/year
Estlink2	4.0
NordBalt	9.2
LitPol link	3.8

4.3. Socioeconomic welfare and congestion income in wholesale power market for the study case

The Table 4.4 represents results from market simulations performed in SF tool for this study case, showing total consumers' and producers' surpluses for the Baltic power system for the year 2020 in each market simulation scenario. The sum of the consumers' and producers' surpluses represents the total socioeconomic welfare. One has to remember that according to the eq. (2.8) it is only the difference between the scenarios which is relevant for the results of this study, so the large absolute values presented for consumers' and producers' surpluses themselves are not to be paid attention to.

Table 4.4. Consumers' and producers' surplus for the market simulation scenarios of the case study

Scenario Nr.	Sum of Consumers' Surplus, [MEUR]	Sum of Producers' Surplus, [MEUR]
1.	66313.3	2634.3
2.	65577.5	2615.3
3.	63795.0	2608.2

By calculating the difference between the scenarios with capacity restrictions (Nr.2 and Nr.3) and the base case scenario (Nr. 1) and dividing these with the amount of hours per year, the average values of socioeconomic welfare decrease per hour of limitations can calculated. For market simulation Scenario Nr.2 (in comparison to Scenario Nr.1), average total socioeconomic welfare decrease is 86160.49 Eur/h. For market simulation Scenario Nr.3 (in comparison to Scenario Nr.1), average total socioeconomic welfare decrease is 290449.4 Eur/h.

Table 4.5 represents results from market simulations performed in the SF tool, showing the congestion income per border (and in total) for the year 2020 for each market simulation scenario.

Table 4.5. Congestion income for various market simulation scenarios

Scenario Nr.	Congestion income, [MEUR]					
	FI-EE /2	EE-LV	LV-LT	LT-SE4 /2	LT-PLA /2	Total
1	32	4	1	27	5	70
2	35	3	0	27	5	71
3	45	1	0	25	7	79

4.4. VOLL estimations

To estimate the losses to customers due to proposed novel LS activations, an average weighted VOLL value for the consumers in the Baltics must be known. In order to calculate that, data on VOLL for the Baltic countries by economy sector presented in [26] and data on EU-27 electricity consumption by sector presented in [92] have been used. [92] is also used to group the VOLL data from [26] into a shortlist of consumption sectors. The summary of these data can be seen in Table 4.6

Table 4.6. Average VOLL by European Environment Agency (EEA) sectors in Baltic countries, EUR/kWh

Consumption division by sectors according to EEA	Average VOLL, EUR/kWh	% of consumption according to EEA
Households	4.8	28.5
Industry	2.9	40.6
Transport	17.5	2.6
Services, agriculture	3.5	28.3

By using data from the Table 4.6 the average weighted VOLL value for the consumers in the Baltics is calculated to be is 4 Eur/kWh.

4.5. The final results of the simulation case

The obtained case study simulation results from the whole Chapter 4 now with help of eq. (2.10), (2.11), (2.13) and (2.14) can be transformed into practical SWR_M, SWR_R, CI and LSC values. These are presented in the Table 4.7. Values for CI are calculated for the average amount of hours per year an isolated island mode of the Baltic power system is expected with the numbers provided in the Chapter 4.2.

Table 4.7. Final economic analysis results for the case study

Case study Nr.	SWR_M, MEUR/year	CI, MEUR/year	SWR_R, MEUR/year	SWR_{total}, MEUR/year	LSC, MEUR/year
1.A.	3.29	-0.005	0.055	**3.340**	**0.040**
1.B.	11.10	-0.039	0.314	**11.375**	
2.A.	3.29	-0.005	0.055	**3.340**	**0.080**
2.B.	11.10	-0.039	0.314	**11.375**	
3.A.	3.29	-0.005	0.055	**3.340**	**0.130**
3.B.	11.10	-0.039	0.314	**11.375**	

The results show that the total reduction of SEW for all scenarios compared to the base case is substantial. The costs of the reserve activation due to the reduction of the cross-border capacities are found to be relatively small, the same is the case for LSC – the costs related to the disconnection of the consumers due to the activation of the novel LS scheme – an important finding which will be further discussed in the discussion chapter.

With these results the condition from the eq. (2.16) is fulfilled for all of the scenarios of the case study which leads to a confirmation of the hypothesis raised in the Introduction chapter.

5. SOCIO-ECONOMIC ASSESSMENT OF THE EFFECT OF THE PROPOSED NOVEL LOAD SHEDDING SCHEME. FORECASTED INPUT DATA.

5.1. General info and definition of study case scenarios

Following the plan for an assessment of the SEW gain of the proposed LS scheme described in the chapter 2.4.4, a second case study/simulation set and an assessment of the SEW will be carried out in this chapter. Similarly to the already executed assessment with historical data in chapter 4, a case study of the socioeconomic welfare gain brought by the proposed novel LS scheme will be executed with Baltic states as a study subject and now by using a forecast of power system and power market data for 2030, 2040 and for 2050 (two cases).

The Table 5.1 shows the simulation set parameters for the power generation sources and the power demand for the four scenario target year groups. As clearly seen the two different scenarios for the year 2050 differ by the amount of the RES present in the scenarios, with scenario 2050_2 having a larger amount of RES in the Baltic power system. All these parameters in the Table 5.1, except for the energy amount/power supply produced by the MEPP, serve as inputs for the simulation set. The energy amount/power supply produced by the MEPP is grid balancing energy and will appear as an outcome/result of each simulation.

Table 5.1. Basic parameters of modelling scenarios

	Parameter	Load/power consumption	SPP	WPP	HPP	sHPP	BPP	PSHPP	MEPP
Scenario		2030							
	Max capacity, MWh/h	6 026	1 489	3 907	1 562	165	522	1 625	4 330
	Annual power demand/supply, TWh	37,86	1,74	11,66	1,90	0,34	3,52	2,85	n/a
Scenario		2040							
	Max capacity, MWh/h	6 629	1 608	4 994	1 562	165	522	1 625	1 500
	Annual power demand/supply, TWh	39,83	1,88	14,90	1,90	0,34	3,52	2,85	n/a
Scenario		2050_1							
	Max capacity, MWh/h	7 233	2 383	7 127	1 562	165	522	1 625	1 500
	Annual power demand/supply, TWh	41,80	2,78	21,26	1,90	0,34	3,52	2,85	n/a

Scenario		2050_2							
	Max capacity, MWh/h	7 233	3 872	11 586	1 562	165	522	1 625	1 500
	Annual power demand/supply, TWh	41,80	4,52	34,57	1,90	0,34	3,52	2,85	n/a

A scenario envelope was defined for this simulation process, based on already mentioned different forecast target years, different MEPP generation prices and simulation model complexity (BPS_MS and BPS_MD) (as both described in the chapter 2.4.3/part 2). The simulation scenario envelope and the resulting case study number overview is presented in the Table 5.2.

Table 5.2. Simulation parameter overview

Target year	MEPP level (low/high)	Simulation model complexity	Case study nr.
2030	L	Simplified	4
		Detailed	5
	H	Simplified	6
		Detailed	7
2040	L	Simplified	8
		Detailed	9
	H	Simplified	10
		Detailed	11
2050_1	L	Simplified	12
		Detailed	13
	H	Simplified	14
		Detailed	15
2050_2	L	Simplified	16
		Detailed	17
	H	Simplified	18
		Detailed	19

The set of transmission capacity restrictions already used in Scenario 3 from the chapter 4.1 is applied to each of these case studies in order to assess the losses in SEW. The overview of transmission capacity parameters with and without restrictions can be seen in the Table 5.3.

Table 5.3. Transmission capacity restriction parameters for the simulation set

Transmission capacity restriction (no/yes)	Transmission line capacity, MWh/h		
	EE ↔ FI	LT ↔ SE4	LT ↔ PL
n	1 016	700	700
y	750	400	400

5.2. Socioeconomic welfare and congestion income in wholesale power market for the study case

The full results of this simulation set are provided in the Annex III. An extraction of the results relevant for the topic of the calculation of the SEW will be provided in this subchapter.

The SEW loss results for each of the case studies show the difference between the SEW of the each case study itself and the same case study with transmission capacity resticrition from the Table 5.3. These SEW loss results are presented in the Table 5.4 together with other simulation results.

Table 5.4. Simulation set results

Case study nr.	Transmission capacity restriction (no/yes)	Market Clearing Price (MCP) , €/MWh	Total import, TWh	Total export, TWh	Social welfare, M€	Social welfare loss, M€
4	n	77.38	13.842	0.993	149,924.287	n/a
	y	91.89	10.129	0.889	149,661.00	-263.287
5	n	78.377	15.975	3.126	149,956.901	n/a
	y	92.890	10.974	1.734	149,681.179	-275.722
6	n	123.97	13.842	0.993	149,069.074	n/a
	y	163.11	10.129	0.889	148,368.78	-700.294
7	n	124.737	15.975	3.126	149,103.193	n/a
	y	164.057	10.974	1.734	148,389.335	-713.858
8	n	77.56	12.755	1.771	157,810.706	n/a
	y	89.26	9.297	1.505	157,744.81	-65.901
9	n	78.723	15.006	2.257	157,857.821	n/a
	y	90.879	10.200	2.408	157,774.402	-83.419
10	n	122.03	12.755	1.771	156,980.089	n/a
	y	154.56	9.297	1.505	156,686.27	-293.818
11	n	123.118	15.006	2.257	157,027.843	n/a
	y	156.126	10.200	2.408	156,716.235	-311.608
12	n	74.20	10.516	4.015	165,812.661	n/a
	y	83.14	7.671	3.097	165,788.57	-24.095
13	n	76.625	12.718	6.217	165,864.613	n/a
	y	86.217	8.567	3.993	165,822.532	-42.081
14	n	111.21	10.516	4.015	165,096.572	n/a
	y	136.58	7.671	3.097	164,913.48	-183.096

15	n	113.520	12.718	6.217	165,149.346	n/a
	y	139.609	8.567	3.993	164,947.550	-201.796
16	n	65.04	6.980	8.397	166,162.064	n/a
	y	71.48	5.161	5.967	166,130.67	-31.392
17	n	70.178	8.891	10.311	166,236.824	n/a
	y	77.637	5.929	6.737	166,191.356	-45.469
18	n	88.22	6.980	8.397	165,720.283	n/a
	y	106.19	5.161	5.967	165,569.46	-150.822
19	n	93.255	8.891	10.311	165,796.906	n/a
	y	112.349	5.929	6.737	165,635.255	-161.650

The most important result from the table is the last column, SW-loss, which corresponds to the $(SW_{Ysx} - SW_{Ysy})$ in the eq. (2.10).

5.3. Miscellaneous assessments towards the final results for the simulation case

5.3.1. Statistics of AC lines outages and major incidents for the study case

The data used for the AC lines outage and major incident rates are identical to the data in the Chapter 4.2.

5.3.2. VOLL estimations

The data used for the VOLL estimation rates are identical to the data in the Chapter 4.4.

5.3.3. Impact of CI on the SWR$_{total}$

The results from the previous test case, Table 4.7, clearly shows that the value of CI is in general negligible compared to both SWR$_M$ and SWR$_R$. Taking account of this fact the CI is going to be excluded from the calculation of the total SEW loss as given by the eq. (2.15).

5.3.4. Calculation of the SWR$_R$

The SWR$_R$ is calculated using the same formula from the eq. (2.11), but assessing the FC_R remains a challenge: as FC_R cannot be directly extracted from the simulation data (as for the simulation with SF in Chapter 4), the values for FC_R have to be approximated from the available simulation set results. For this purpose the average import reduction for each case study will be taken from the overall simulation results and divided by the yearly amount of hours, 8760 h. For simplified models the average total import reduction for each case study will be taken, for detailed models the sum of average import reduction only from Finland and Sweden will be taken as only interconnectors with these countries are affected in the case of islanding of the Baltic power system.

The values for the P_R for this simulation set will be set by the prices for the MEPP as given in the Chapter 2.4.3 – 120 or 240 EUR/MWh as the low and high MEPP price levels as given by the Table 5.2.

5.3.5. LSC estimation

The data used for the LSC estimation will be equal to the numbers used for the case studies 3A and 3B from the Chapter 4, as only the amount of LS in these scenarios is plausible for the future power system situation of the Baltic power grid with substantial amounts of RES and therefore also low inertia levels in the power system.

5.4. The results

Taking the simulation set results for this case study from the Table 5.4 and using all the necessary data provided by the Chapters 4.2, 4.4 and the eq. (2.10), (2.11), and (2.14) the final SEW loss results are obtained for this case study/simulation set, it can be seen in Table 5.5.

Table 5.5. Final economic analysis results for the case study

Case study nr.	SWR_M, MEUR/year	SWR_R, MEUR/year	SWR_{total}, MEUR/year	LSC, MEUR/year
4	1.14	0.44	1.58	
5	1.20	0.51	1.71	
6	3.04	0.87	3.91	
7	3.10	1.02	4.12	
8	0.29	0.41	0.70	
9	0.36	0.49	0.85	
10	1.28	0.81	2.09	
11	1.35	0.97	2.32	0.13
12	0.10	0.33	0.43	
13	0.18	0.42	0.60	
14	0.80	0.70	1.50	
15	0.88	0.83	1.71	
16	0.14	0.21	0.35	
17	0.20	0.31	0.51	
18	0.66	0.43	1.09	
19	0.70	0.61	1.31	

The results show that for all case studies in the simulation set the total SEW sees a reduction when compared to the base case. For some of the case studies this reduction is relatively low and for some it reaches million EUR magnitude. The costs of the reserve activation, SWR_R, for this simulation set are found to comprise a substantial part of the overall SEW reduction.

The same way as for the previous simulation set, the costs for LSC – the costs related to the disconnection of the consumers due to the activation of the novel LS scheme – are for all case studies lower than the total SEW reduction.

With these results the condition from the eq. (2.16) <u>is again fulfilled</u> for all of the of the case studies which again leads to a confirmation of the hypothesis raised in the Introduction chapter.

6. DISCUSSION

The hypothesis in the very beginning of the thesis established three main goals for this scientific work:
- introduce a concept of a novel load-shedding scheme based on the usage of SC as a frequency sensor;
- show that implementation of this proposed LS scheme into the Baltic power grid would substantially improve the frequency stability of the grid after the ENTSO-E synchronization;
- show that implementation of this proposed LS scheme into the Baltic power grid would substantially increase the SEW for the grid users.

The concept of a novel load shedding scheme was introduced and described, with basic operating principles and some technical details for possible operating logic given. An implementation of such a LS scheme into a practical power system is not considered to be a challenging task, given that the SC are present/installed in the grid. The proposed LS arrangement is less about hardware upgrades and more about changing systems operation logics in the frequency emergency states. The TSOs of, f.ex. Baltic power system, could install the proposed LS arrangement relatively quickly and with negligible investments. The bigger question with the implementation of this LS scheme is a de-facto acceptance of load shedding itself as a measure for frequency stabilization. In the Baltic power system the historic cases of real usage of UFLS are absent – that is the UFLS scheme is present in the grid but due to the vast inertia and frequency resources of the UPS synchronous power system, to which Baltic are currently synchronously connected, this existing UFLS has never been activated. This means that the planned synchronization to the ENTSO-E area and the following possible island mode operation of the Baltic power grid brings a fundamental shift into the operation philosophy of the Baltic power system. When LS activation is a non-existing experience for TSOs, the threshold of accepting LS (basically disconnection of grid users) becomes high. On the other hand, denying the LS place in the system operation logics can probably lead to frequency related blackouts/brownouts – and as a fallout of such an event a LS scheme as integral part of operational logics will be accepted sooner or later. A change in the operational approach will be a challenge for the affected TSOs.

To prove the effect of the proposed novel LS scheme on the frequency stability of the Baltic system in the island mode, two test case/simulation sets were executed. Both presented test case sets demonstrated the difference in frequency response between the existing UFLS scheme and the proposed novel LS scheme – in the favor of the proposed novel LS scheme. The principal result of these simulations is: if Baltic power system would get the proposed LS scheme installed, the frequency deviations in the case of severe loss-of-generation event during an island mode of operation will be substantially reduced. With other words – the frequency stability of the system in island mode is greatly improved if the proposed LS scheme is installed. Three out of four scenarios (A, C, D) in first test case set did show a substantial improvement of frequency stability comparing to usage of the existing UFLS scheme. The positive effect the proposed LS scheme had on the frequency came with a very strong correlation with decreasing

system inertia, meaning that this novel LS scheme can and will become crucial for system frequency stability taking account of the ongoing developments of growing shares of the RES in the power system and decreasing system inertia levels.

The fourth scenario (B) in first test case set did even show a full supremacy of the proposed novel LS scheme over the existing UFLS arrangement because in that particular scenario the existing UFLS scheme was not even triggered, while the proposed LS scheme was activated as planned and did substantially reduce the fall of system frequency. For this particular scenario here one can argue – how a situation with load shedding/disconnection of consumers is a better situation than one where no load is shed? My argument is that a controlled load shedding and control of the frequency is a better option than an uncontrolled frequency fall below safe threshold of 49 Hz and all the potential cascading disconnection effects this may bring.

The second test case set of the frequency stability case study demonstrated again the superiority on the proposed LS scheme over existing/conventional UFLS arrangement. But the main focus of this test case set was to examine how a change in the gain coefficient of the proposed LS scheme affects the frequency response of the system during a major loss-of-generation event. The finding is – the larger K is introduced (more load is disconnected), the higher is the value for the frequency nadir and thus – the smaller frequency fall/higher stability is achieved. However, a healthy trade-off between the frequency stability margins and the volume of load to be shed must be found. This is a question each TSO must figure out before their potential implementation of the proposed LS arrangement. This particular topic will become important for the TSOs during the practical implementation of the proposed LS scheme and will play a role in the determination of the practical sensitivity of the LS scheme in operation.

After showing a substantial positive effect on the system frequency, an economic assessment of the impact of the proposed LS scheme onto the SEW had to be made to cement the arguments for the introduction of the scheme. This assessment was made on two different sets of simulations/case studies with a fundamental difference – usage of either historic or forecasted power system input data. The fundamental difference in the approaches for the two is simple – historic data simulations have known inputs but also the results apply to the past and thus do not describe the future well; while the opposite is true for the forecasted data simulations – the input data is a forecast/guess and the results describe the future only as well as precise the input data forecasts are.

The simulations with historic input data were made taking the year 2020 as the base year for the data input. One can consider the year 2020 in the Baltic power system to be a time when the presence of the conventional power plants was still strong and the development of RES still at early stage. As the conventional power plants in the Baltics have always been mostly fossil fuel fired, they rank quite high up in a typical merit-order of generators. Renewable and other CO_2-neutral sources like hydro power and nuclear power plants are usually placed in the lower part of a typical merit-order of generators due to the non-existing/low fuel costs and CO_2-costs. The logical consequence of these facts is a large power import volumes from the Nordic countries into the Baltic power system, as the main power sources in the Nordics are hydro and nuclear power plants. This means the year 2020 represents a typical historical situation with

large imports of electricity from price areas with relatively low power prices. The simulations with forecasted input data for years 2030, 2040 and 2050 on the other hand assume large generating capacities of RES, mostly wind and solar power plants, and thus – large quantities of cheap power in the lower part of a typical generator merit-order. This fact consequentially leads to less imports into the Baltic power system. This means that the simulation set with forecasted data represent a situation with small or no imports of power and even exporting power at some periods of time. This is a highly important mark to take notice of: the presented simulation data from both simulation sets present a kind of continuum for years 2020-2030-2040-2050 with a steady, gradual movement from a system with large imports to a system with non-imports or even significant power exports.

The most important result of the simulations with historical data for 2020 was that it resulted in an annual reduction of SEW of around 11.4 MEUR for a system with proposed novel LS scheme installed versus a system with the continued usage of the present UFLS scheme. The simulations with forecasted input data showed a range of values for the reduction of the SEW for the years 2030-2040-2050, a range of everything between ca. 0.4-4.1 MEUR annually. It was clearly seen that the numbers in that range were greatly affected by the marginal price of MEPP and by the amount of RES generation capacity available, meaning numbers were affected by the amount of cheap renewable energy in the system. So, the high MEPP marginal prices gave high annual reduction of SEW, and lower amount of RES capacity also gave higher annual reduction of SEW. Both high MEPP marginal prices and low RES capacity mean high imports of power into the Baltics, so reducing the cross-border transmission capacities, which is a consequence of not implementing the proposed novel LS scheme, lifts the SEW to extra high levels as the import capacity is restricted exactly when the necessity for power imports is high.

The amounts presented for the annual SEW reduction for the Baltic power system may seem small in the overall context of the total costs for consumers and generators, but I would argue they are still of considerable dimension. Looking from a fiscal point of view only: millions of EUR saved annually is a significant contribution and is, in my opinion, a saving worth achieving, especially when an improved power system frequency stability comes along as a significant bonus. Looking from a technical point of view: the proposed system improves system frequency stability and cuts down the risks of blackouts and is therefore absolutely worth investing into no matter how small the fiscal gain is. And in my opinion the TSOs who will potentially consider introduction of the proposed LS scheme will firstly assess the positive impact on the system frequency stability and then consider the fiscal SEW gain only as a secondary factor.

All in all, the proposed novel LS scheme has been proved to deliver major both system stability-related and fiscal gains to power grids as displayed in the thesis' test cases/ simulations.

CONCLUSIONS

1. The hypothesis of the thesis has been proven and the objective of thesis has been achieved. The proposed novel LS scheme, based on the usage of SC as a frequency sensor, does substantially improve the frequency stability and increases the SEW of a weakly interconnected or a low-inertia power system. The whole range of case studies carried out during the thesis has proven those statements.

2. The tasks of the thesis have been successfully carried out:
   - A theoretical background and motivation for introduction of the proposed novel LS scheme were explained. An explanation on the fundamental novelty of the proposal – usage of SC as ROCOF sensors – was given and advocated. Further, the detailed methods and concepts for the proposed LS scheme were introduced.
   - A grid-stability related motivation for an introduction of the proposed LS scheme was given.
   - An economic/fiscal motivation for an introduction of the proposed LS scheme was given.

3. A series of case studies/simulations to measure the effect of the proposed LS scheme on power system stability were conducted. The case studies showed in unison a major positive effect of the proposed LS scheme on the frequency stability of the given power system when comparing to the present UFLS schemes. The proposed LS scheme showed an ability to limit power system frequency fall in cases of major loss-of-generation contingencies and hold the frequency above the dangerous blackout threshold of 49 Hz. The detected positive effect of the proposed LS scheme had a strong direct correlation with decreasing power system inertia levels.

4. A series of case studies/simulations to measure the effect of the proposed LS scheme on power systems SEW were conducted. The case studies showed positive effect of the proposed LS scheme on the SEW of the Baltic power system operating in an island mode after their desynchronization from the UPS/IPS grid when comparing to the situation when the scheme is not introduced. The measured positive effect on the SEW is in the magnitude of millions of EUR for most of the studied scenarios. The detected measured positive effect on the SEW had a strong direct correlation with increased power imports into the Baltic power system.

REFERENCES

[1]   UN Framework Convention on Climate Change, *The Paris Agreement,* 2016.

[2]   International Renewable Energy Agency, «World Energy Transitions Outlook - 1.5°C Pathway, Preview,» 2021.

[3]   International Energy Agency, «Seven Key Principles for Implementing Net Zero» 2021.

[4]   ENTSO-E, «TYNDP 2020 - Completing the map. Power system needs in 2030 and 2040.» ENTSO-E, Brussels, 2021.

[5]   ENTSO-E, «Nordic report - Future system inertia.,» ENTSO-E, Brussels, 2018.

[6]   European Commision, *Energy security: The synchronisation of the Baltic States' electricity networks - European solidarity in action; press release,* Brussels, Belgium, 2019.

[7]   H. T. Nguyen, G. Yang, A. H. Nielsen and P. Højgaard Jensen, «Combination of Synchronous Condenser and Synthetic Inertia for Frequency Stability Enhancement in Low-Inertia Systems» *IEEE Transactions on sustainable energy,* vol. 10, iss. 3, 2019.

[8]   A. Stiger, R. A. Rivas and M. Halonen, «Synchronous Condensers Contribution to Inertia and Short Circuit Current in Cooperation with STATCOM» *2019 IEEE PES GTD Grand International Conference and Exposition Asia (GTD Asia)*, Bangkok, Thailand, 2019.

[9]   R. W. Kenyon, A. Hoke, J. Tan, B. Kroposki and B.-M. Hodge, «Grid-Following Inverters and Synchronous Condensers: A Grid-Forming Pair?» *2020 Clemson University Power Systems Conference (PSC)*, Clemson, USA, 2020.

[10] M. Nedd, C. Booth and K. Bell, «Potential solutions to the challenges of low inertia power systems with a case study concerning synchronous condensers» *52nd International Universities Power Engineering Conference (UPEC)*, Heraklion, Greece, 2017.

[11] J. Machowski, J. W. Bialek and J. R. Bumby, Power System Dynamics, 2 red., John Wiley & Sons, 2008, p. 171.

[12] A. Sauhats, A. Utans, J. Silinevics, G. Junghans and D. Guzs, «Enhancing Power System Frequency with a Novel Load Shedding Method Including Monitoring of Synchronous Condensers' Power Injections» *Energies,* vol. 14, iss. 5, 2021.

[13] DNV GL, «RoCoF Alternative Solutions Technology Assessment - FINAL REPORT PHASE 1» 2015.

[14] AS Augstsprieguma Tīkls*, Personal communication,* Riga, Latvia, 2020.

[15] C. Payerl, «Introduction to ABB Synchronous Condenser offering - A solution to improve grid strength,» 2020. [Website]. Available: https://library.e.abb.com/public/1fb2ec9a1eb34241924f030f47048951/Syncon_webinar__2020 _Dec_presented_2020DEC.pdf. [Accessed 24 July 2022].

[16] C. Szaba, «Synchronous condensers. An old tool rediscovered to address new grid challenges.» *Power Engineering International,* nr. 11, 2017.

[17] A. Moser, Planung und Betrieb von Elektrizitätsversorgungssytemen, Skriptum zur Vorlesung., Aachen: IAEW, 2012, pp. 151-153.

[18] W. Huang, J. Yu, Z. Yuan, Z. He, J. He and M. Deng, «An adaptive under-frequency optimal control strategy for power system combined pumped storage and under-frequency load shedding.,» *PLOS ONE,* vol. 16, iss. 12, 2021.

[19] B. Delfino, S. Massucco, A. Morini, P. Scalera and F. Silvestro, «Implementation and comparison of different under frequency load-shedding schemes.» *Power Engineering Society Summer Meeting*, New York, U.S., 2001.

[20] U. Rudez and R. Mihalic, «Comparison of adaptive UFLS schemes in modern power systems.» *IEEE Electrical Power & Energy Conference*, San Diego, CA, U.S., 2010.

[21] K. Ben Kilani, M. Elleuch and A. H. Hamida, «Dynamic under frequency load shedding in power systems.» *14th International Multi-Conference on Systems, Signals & Devices (SSD)*, Marrakech, Morocco, 2017.

[22] F. Zare, A. Ranjbar and F. Faghihi, «Intelligent topology-oriented load shedding scheme in power systems.» *27th Iranian Conference on Electrical Engineering (ICEE)*, Yazd, Iran, 2019.

[23] Z. Jianjun, S. Dongyu, Dong Z. and G. Yang, «Load Shedding Control Strategy for Power System Based on the System Frequency and Voltage Stability.» *China International Conference on Electricity Distribution (CICED)*, Tianjin, China, 2018.

[24] M. Talaat, A. Hatata, A. S. Alsayyari and A. Alblawi, «A smart load managementb system based on the grasshopper optimization algorithm using the under-frequency load shedding approach.» *Energy,* vol. 190, 2020.

[25] U. Rudez and R. Mihalic, «Trends in WAMS-based under-frequency load shedding protection. In Proceedings of the» *IEEE EU-ROCON 2017-17th International Conference on Smart Technologies*, Ohrid, Macedonia, 2017.

[26] ACER, «Study on the estimation of the value of lost load of Electricity supply in Europe. Final report.» ACER, Brussels, 2018.

[27] L. Hirth, «The Merit Order Model and Marginal» 2 September 2022. [Website]. Available: https://neon.energy/marginal-pricing. [Accessed 19 February 2023].

[28] ENTSO-E, «2nd ENTSO-E Guideline For Cost Benefit Analysis of Grid Development Projects» 2018.

[29] NordPoolSpot, «Curtailment, price thresholds and decoupling,» [Website]. Available: https://www.nordpoolgroup.com/en/trading/Day-ahead-trading/Curtailment-price-thresholds-and-decoupling/. [Accessed 24 August 2022].

[30] NordPoolSpot, «EUPHEMIA Public Description,» [Website]. Available: https://www.nordpoolgroup.com/globalassets/download-center/single-day-ahead-coupling/euphemia-public-description.pdf. [Accessed 24 August 2022].

[31] N-Side, «Public presentation of Euphemia description and functioning» [Website]. Available: https://www.n-side.com/wp-content/uploads/2017/08/Euphemia-Public-Presentation.pdf. [Accessed 23 May 2021].

[32] European Commision, «The Baltic Power System Between East and West Interconnections, JRC Science for Policy Report» Brussels, Belgium, 2016.

[33] NordPoolSpot, [Website]. Available: https://www.nordpoolgroup.com. [Accessed 15 December 2020].

[34] G. Junghans, A. Silis, K. Marcina and K. Ertmanis, «Role of Balancing Markets in Dealing with Future Challenges of System Adequacy Caused by Energy Transmission» *Latv. J. Phys. Tech. Sci.,* vol. 57, p. 48–56, 2020.

[35] European Union, «2030 Climate & Energy Framework» Brussels, Belgium, 2020.

[36] Republic of Estonia, «Estonia's 2030 National Energy and Climate Plan» Tallinn, Estonia, 2019.

[37] Republic of Latvia, «Latvia's National Energy and Climate Plan 2021-2030» Riga, Latvia, 2020.

[38] Republic of Lithuania, «National Energy and Climate Action Plan of the Republic of Lithuania for 2021-2030» Vilnius, Lithuania, 2021.

[39] P. Ivanova, A. Sauhats and O. Linkevics, «Towards optimization of combined cycle power plants' start-ups and shut-down» *57th International Scientific Conference on Power and Electrical Engineering of Riga Technical University (RTUCON)*, Riga, Latvia, 2016.

[40] AS Augstsprieguma Tikls, «MK DOD ZAĻO GAISMU AST IEGĀDĀTIES, PĀRVALDĪTUN EKSPLUATĒT ELEKTROENERĢIJAS AKUMULĀCIJASIEKĀRTAS JEB BATERIJAS» [Website]. Available: https://www.ast.lv/lv/events/mk-dod-zalo-gaismu-ast-iegadaties-parvaldit-un-ekspluatet-elektroenergijas-akumulacijas. [Accessed 23 February 2023].

[41] S. Kiene, O. Linkevics, K. Gicevskis and E. Groza, «Modelling of Battery Energy Storage System Providing FCR in Baltic Power System after Synchronization with the Continental Synchronous Area,» *Energies,* vol. 15, iss. 11.

[42] SDAC, «Information on Single Day-ahead Coupling (SDAC)» [Website]. Available: https://www.entsoe.eu/network_codes/cacm/implementation/sdac/. [Accessed 23 May 2021].

[43] S. Kovalenko and S. Rubcovs, «Rebuilding or Upgrading of the Existing Under Frequency Load Shedding System of Baltic States» *IEEE 63th International Scientific Conference on Power and Electrical Engineering of Riga Technical University (RTUCON)*, Riga, 2022.

[44] D. Guzs, A. Utans, A. Sauhats, G. Junghans un J. Silinevics, «Resilience of the Baltic power system when operating in island mode» *IEEE 61th International Scientific Conference on Power and Electrical Engineering of Riga Technical University (RTUCON)*, Riga, Latvia, 2020.

[45] A. Rubio, H. Behrends, S. Geissendorfer, K. von Maydell and C. Agert, «Determination of the Required Power Response of Inverters to Provide Fast Frequency Support in Power Systems with Low Synchronous Inertia» *Energies,* vol. 13, iss. 816, 2020.

[46] A. Sauhats, I. Svalova, A. Svalovs, D. Antonovs, A. Utans and G. Bochkarjova, «Two-terminal out-of-step protection for multi-machine grids using synchronised measurement» *IEEE Eindhoven PowerTech*, Eindhoven, The Netherlands, 2015.

[47] A. Sauhats, A. Utans, D. Antonovs, and A. Svalovs, «Angle Control-Based Multi-Terminal Out-of-Step Protection System,» *Energies,* vol. 10, iss. 308, 2017.

[48] I. B. Sperstad, O. Wolfgang, T. I. Reigstad and G. H. Kjolle, «Probabilistic socio-economic cost assessment integrating power market and reliability analysis,» *IEEE International Conference on Probabilistic Methods Applied to Power Systems (PMAPS)*, Boise, ID, USA, 2018.

[49] Energy Ministry of the Republic of Lithuania, «LitPol Link» [Website]. Available: https://enmin.lrv.lt/en/strategic-projects/electricity-sector/electricity-link-litpol-link. [Accessed 9 July 2021].

[50] Polskie Sieci Energetyczne (PSE), «Uroczyste otwarcie nowych obiektów przesyłowych zrealizowanych w ramach Projektu budowy mostu elektroenergetycznego Polska – Litwa» [Website]. Available: https://www.pse.pl/-/uroczyste-otwarcie-nowych-obiektow-przesylowych-zrealizowanych-w-ramach-projektu-budowy-mostu-elektroenergetycznego-polska-8211-litwa. [Accessed 25 August 2022].

[51] L. Wenyuan, Risk Assessment of Power Systems. Models, Methods, and Applications., JOHN WILEY & SONS INC, 2014.

[52] A. A. Chowdhury and D. O. Koval, «Deregulated Transmission System Reliability Planning Criteria Based on Historical Equipment Performance Data» *IEEE Transactions on Industry Applications,* vol. 37, iss. 1, 2001.

[53] A. A. Chowdhury and D. O. Koval, «Assessment of Transmission-Line Common-Mode, Station-Originated, and Fault-Type Forced-Outage Rates» *IEEE Transactions on Industry Applications,* vol. 46, iss. 1, 2010.

[54] Ю. Н. Балаков, М. Ш. Мисриханов and А. В. Шунтов, Проектирование схем электроустановок., ЗАО "Издательский дом МЭИ", 2004.

[55] Е. Н. Ефимов, Л. В. Тимашова and Н. В. Ясинская, «ПРИЧИНЫ И ХАРАКТЕР ПОВРЕЖДАЕМОСТИ КОМПОНЕНТОВ ВОЗДУШНЫХ ЛИНИЙ ЭЛЕКТРОПЕРЕДАЧИ НАПРЯЖЕНИЕМ 110-750 кВ В 1997-2007 ГГ.» *ЭНЕРГИЯ ЕДИНОЙ СЕТИ,* vol. 5, iss. 5, 2012.

[56] ENTSO-E AISBL, «Nordic and Baltic Grid Disturbance Statistics 2019. Regional Group Nordic.» 22 September 2020. [Website]. Available: https://eepublicdownloads.blob.core.windows.net/public-cdn-container/clean-documents/Publications/SOC/Nordic/Nordic_and_Baltic_Grid_Disturbance_Statistics_2018.pdf. [Accessed 13 July 2021].

[57] NordPoolSpot, «Urgent Market Messages (UMM)» [Website]. Available: https://umm.nordpoolgroup.com/. [Accessed 25 August 2022].

[58] ENTSO-E, «Single Day-ahead Coupling (SDAC)» [Website]. Available: https://www.entsoe.eu/network_codes/cacm/implementation/sdac/. [Accessed 9 October 2022].

[59] SDAC, «Single Day-ahead Coupling (SDAC)» [Website]. Available: https://www.entsoe.eu/network_codes/cacm/implementation/sdac. [Accessed 11 July 2021].

[60] Nord Pool AS, «Historical Market Data» [Website]. Available: https://www.nordpoolgroup.com/historical-market-data. [Accessed 11 July 2021].

[61] R. Petrichenko, J. Kozadajevs, L. Petrichenko and A. Silis, «Reserve power estimation according to the Baltic power system 2050 development plan,» *ENERGYCON 2022 - 2022 IEEE 7th Int. Energy Conference*, 2022.

[62] R. Petricenko, A. Sauhats, K. Baltputnis, Z. Broke and L. Petrichenko, «Modelling the Future of the Baltic Energy Systems: A Green Scenario,» *Latvian Journal of Physics and Technological Sciences,* vol. 58, iss. 3, pp. 47-65, 2021.

[63] R. Petrichenko, L. Petrichenko, O. Ozgonenel and R. Komarovs, «The assessment of long-term import-export capabilities of Baltic power system,» *IEEE 62nd International Scientific Conference on Power and Electrical Engineering - RTUCON 2021*, 2021.

[64] MathWorks, «linprog - solve linear programming problems» [Website]. Available: https://www.mathworks.com/help/optim/ug/linprog.html.

[65] MathWorks, «fmincon-Find minimum of constrained nonlinear multivariable function» [Website]. Available: https://se.mathworks.com/help/optim/ug/fmincon.html.

[66] MathWorks, «narxnet-Nonlinear autoregressive neural network with external input» [Website]. Available: https://se.mathworks.com/help/deeplearning/ref/narxnet.html.

[67] L. Petrichenko, A. Sauhats, R. Petrichenko and D. Bezrukovs, «Long-Term Price Forecasting for the Cost-Benefit Analysis of Power Equipment» IEEE 59th International Scientific Conference on Power and Electrical Engineering of Riga Technical University (RTUCON), 2018.

[68] L. Petrichenko, Z. Broka, A. Sauhats and D. Bezrukovs, «Cost-Benefit Analysis of Li-Ion Batteries in a Distribution Network» *15th International Conference on the European Energy Market (EEM)*, Lodz, Poland, 2018.

[69] R. Petrichenko, L. Petrichenko, A. Sauhats, A. Slivikas, S. Gudzius and M. Zima-Bockarjova, «Profitability Study of Floating PV and Storage Pumped Hydropower Plant» *17th International Conference on the European Energy Market (EEM)*, Stockholm, Sweden, 2020.

[70] R. Petrichenko, L. Petrichenko, K. Baltputnis, A. Sauhats, S. Gudzius and A. Slivikas, «Selection of the initial state and duration of the planning period in the tasks of managing energy storage systems» *IEEE 61th International Scientific Conference on Power and Electrical Engineering of Riga Technical University (RTUCON)*, Riga, Latvia, 2020.

[71] I. Moshkin and A. Sauhats, «Solving district heating problems by using cooperative game theory methods» *IEEE 16th International Conference on Environment and Electrical Engineering (EEEIC)*, Florence, Italy, 2016.

[72] E. Grebesh, O. Linkevics and P. Ivanova, «Optimisation of Combined Cycle Gas Turbine Power Plant in Intraday Market: Riga CHP-2 Example» *Latvian Journal of Physics and Technical Sciences,* vol. 55, iss. 1, 2018.

[73] R. Oleksijs, A. Sauhats and B. Olekshii, «Generator cooperation in district heating market considering open electricity market» *IEEE 61th International Scientific Conference on Power and Electrical Engineering of Riga Technical University (RTUCON)*, Riga, Latvia, 2020.

[74] A. Sauhats, R. Petrichenko, K. Baltputnis, Z. Broka and R. Varfolomejeva, «A multi-objective stochastic approach to hydroelectric power generation scheduling» *2016 Power Systems Computation Conference (PSCC)*, Genoa, Italy, 2016.

[75] A. Sauhats, R. Petrichenko, Z. Broka, K. Baltputnis and D. Sobolevskis, «ANN-based forecasting of hydropower reservoir inflow» *57th International Scientific Conference on Power and Electrical Engineering of Riga Technical University (RTUCON)*, Riga, Latvia, 2016.

[76] R. Petrichenko, K. Baltputnis, D. Sobolevsky and A. Sauhats, «Estimating the Costs of Operating Reserve Provision by Poundage Hydroelectric Power Plants» *15th International Conference on the European Energy Market (EEM)*, Lodz, Poland, 2018.

[77] I. Diahovchenko, L. Petrichenko, I. Borzenkov and M. Kolcun, «Application of photovoltaic panels in electric vehicles to enhance the range» *Heliyon,* vol. 8, iss. 12.

[78] J. Kozadajevs, R. Petrichenko, O. Ozgonenel, D. Boreiko, A. Dolgicers and L. Petrichenko, «Assessment of PV Integration in the Industrial and Residential Sector under Energy Market Conditions» *Latvian Journal of Physics and Technical Sciences,* vol. 58, iss. 3, pp. 82-97.

[79] A. Sauhats, R. Petrichenko, L. Petrichenko, A. Silis and R. Komarovs, «The assessment of the impact of electric vehicles on the power balance of the Baltic energy system» *IEEE 62nd International Scientific Conference on Power and Electrical Engineering of Riga Technical University (RTUCON)*, Riga, Latvia, 2021.

[80] M. Zima-Bockarjova, A. Sauhats, L. Petrichenko and R. Pertichenko, «Shapley-Value-Based Charging and Discharging Scheduling for Electric Vehicles in a Parking Station» *IEEE 60th International Scientific Conference on Power and Electrical Engineering of Riga Technical University (RTUCON)*, Riga, Latvia, 2019.

[81] ENTSO-E, «Transparency platform,» [Website]. Available: https://transparency.entsoe.eu/transmission-domain/r2/dayAheadPrices/show. [Accessed 19 February 2023].

[82] SKM Market Predictor AS, «Long-Term Power Outlook 2019.» [Website]. Available: https://www.skmenergy.com/reports/long-term-power-outlook.

[83] Nord Pool AS, «Day-ahead market» [Website]. Available: https://www.nordpoolgroup.com/the-power-market/Day-ahead-market.

[84] LVGMC, «LVGMC, "Latvian Environment, Geology and Meteorology Centre,",» [Website]. Available: https://videscentrs.lvgmc.lv/.

[85] Litgrid AB, «Scenario Building for the Evolution of Lithuanian Power Sector for 2020 - 2050.» [Website]. Available: https://lsta.lt/wp-content/uploads/2020/12/201217-Scenario-building-for-Lithuanian-electric-power-sector_final-report.pdf.

[86] M. Neeme, «The future of the Estonian energy sector in relation to EU 2050 low carbon economy roadmap» [Website]. Available: https://stud.epsilon.slu.se/9368/1/neeme_m_160706.pdf.

[87] Estonian Parliament, «Resolution of the Riigikogu. General Principles of Climate Policy until 2050» [Website]. Available: https://ec.europa.eu/clima/sites/lts/lts_ee_et.pdf.

[88] Republic of Estonia, «Estonia's 2030 National Energy and Climate Plan (NECP 2030)» [Website]. Available: https://faolex.fao.org/docs/pdf/est200007.pdf.

[89] European Commission, «European Commission, 2050 long-term strategy» [Website]. Available: https://ec.europa.eu/clima/policies/strategies/2050_en#tab-0-0.

[90] The Republic of Latvia, «Strategy of Latvia for the Achievement of Climate Neutrality by 2050» [Website]. Available: https://ec.europa.eu/clima/sites/lts/lts_lv_en.pdf.

[91] NordPool AS, «Day-ahead Market, Nordic/Baltic Market and CE Market» 10 January 2023. [Website]. Available: https://www.nordpoolgroup.com/48e8b6/globalassets/download-center/rules-and-regulations/day-ahead-market-regulations-sdac-10.01.2023.pdf.

[92] European Environment Agency, «Final electricity consumption by sector, EU-27.» [Website]. Available: https://www.eea.europa.eu/data-and-maps/figures/final-electricity-consumption-by-sector-eu-27 . [Accessed 10 October 2022].

[93] U.S. Department of Energy, «Factors Affecting PMU Installation Costs» 2014.

[94] Siemens Power Technologies Inc., *PSS/E-34 Program Operational Manual,* New York, NY, USA, 2019.

[95] Operation Technology Inc., *ETAP Products & Solutions Comprehensive, Integrated Suite of Power System Software Modules from Design to Operation,* Irvine, CA, USA, 1995.

[96] European Commission, «Commission Regulation (EU) 2017/1485 of 2 August 2017 establishing a guideline on electricity transmission system operation» [Website]. Available: https://eur-lex.europa.eu/legal-content/EN/TXT/?uri=CELEX%3A32017R1485. [Accessed 13 October 2022].

[97] MathWorks, «intlinprog - Mixed-integer linear programming (MILP),» [Website]. Available: https://se.mathworks.com/help/optim/ug/intlinprog.html.

ANNEXES

Import price forecasts used in the power market simulations with forecasted input data (chapter 5)

Poland 2030 hourly electricity market price prediction.
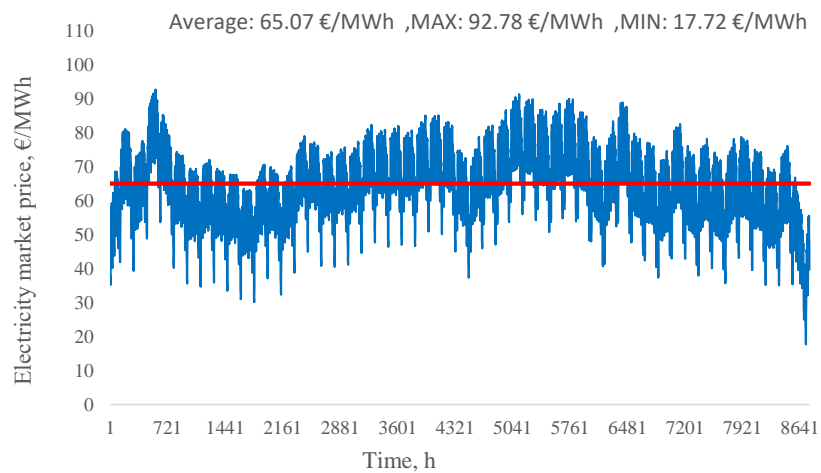
Sweden 2030 hourly electricity market price prediction.

Average: 65.07 €/MWh ,MAX: 92.78 €/MWh ,MIN: 17.72 €/MWh

Average: 42.06 €/MWh ,MAX: 80.20 €/MWh ,MIN: 11.74 €/MWh
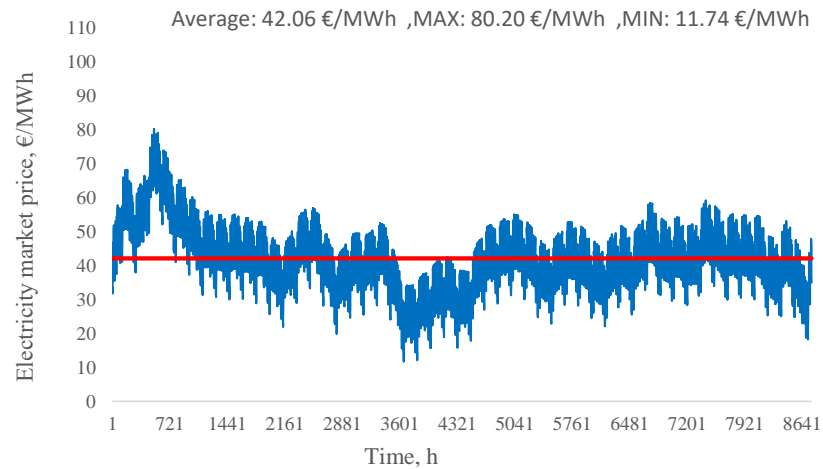
Finland 2030 hourly electricity market price prediction.
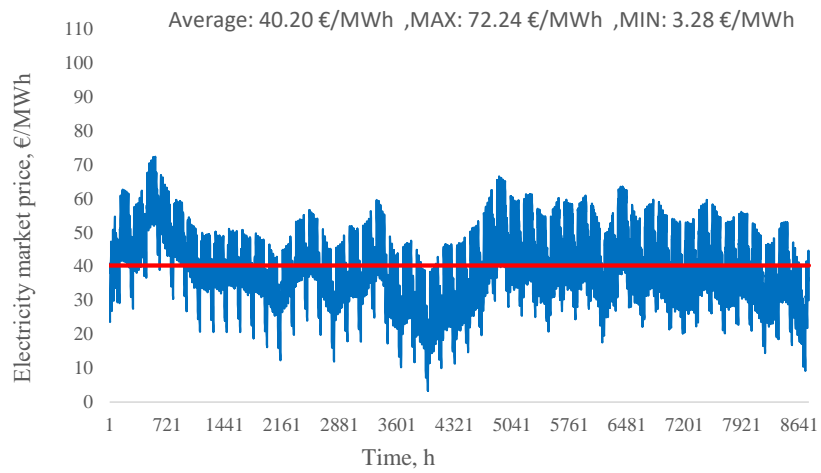
BPS price forecasts used in the power market simulations with forecasted input data (chapter 5)

BPS 2030 hourly electricity market price prediction.
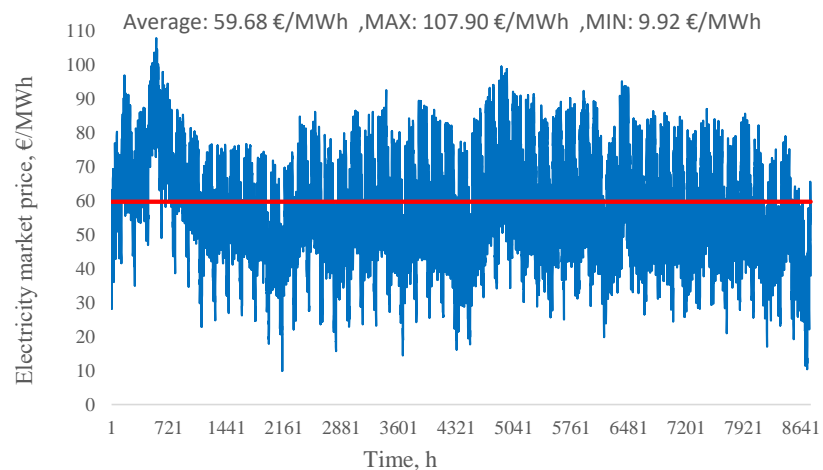
BPS 2040 hourly electricity market price prediction.
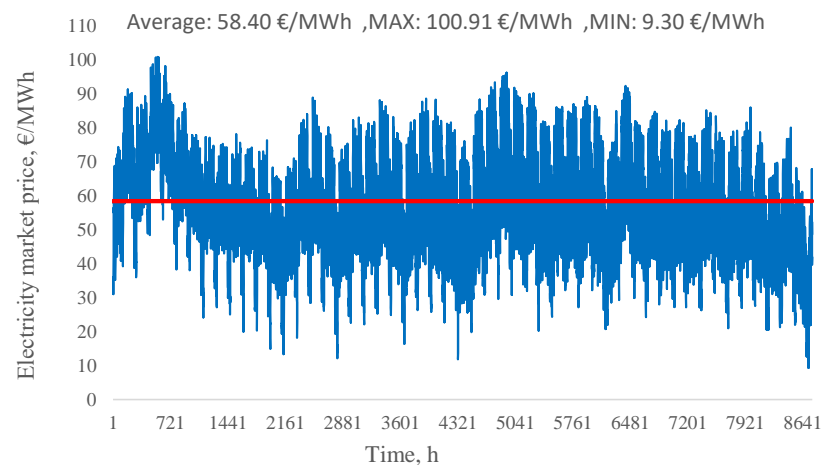
BPS 2050 hourly electricity market price prediction.

Average: 59.91 €/MWh ,MAX: 105.25 €/MWh ,MIN: 10.57 €/MWh
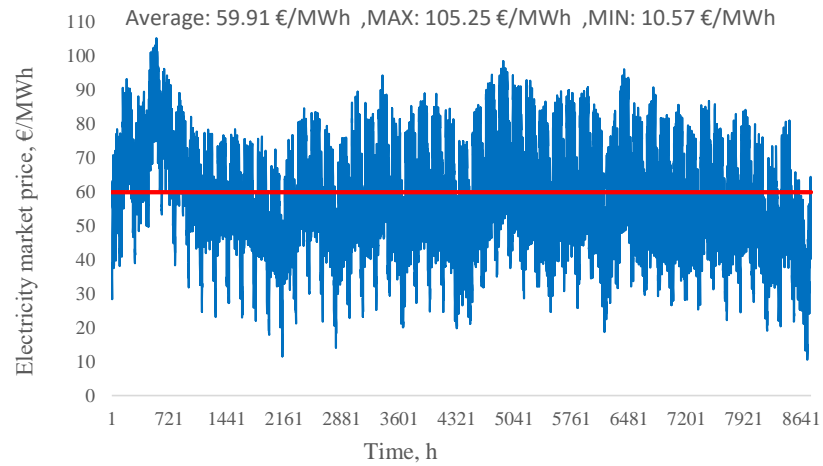
Full results of the SEW simulations with forecasted input data (chapter 5)

NAME	Market Clearing Price (MCP), €/MWh	DELTA of MCP, €/MWh, %		Demand area, M€	Supply area, M€	Social Welfare, M€	DELTA of Social Welfare, M €, %		Total, TWh	Peak, MWh	Total, TWh	Peak, MWh	Total, TWh	Frequency, %	Peak, MWh	Fi	SE4	PL	TOTAL	Fi	SW	PL	TOTAL
2030						**2030**																	
SIMPLIFIED_S_1	77.38			151,459.880	1,535.594	149,924.287			37.865	6,025.590	22.012	8,468.00	3.037	38.77%	2,740.00				13.842				0.993
SIMPLIFIED_S_1_mod	91.89	14.511	18.75%		1,798.881	149,661.00	-263.287	-0.18%					6.750	59.35%	3,606.00				10.129				0.889
DETAILED_S_1	78.377			151,459.880	1,502.979	149,956.901			37.865	6,025.590	22.012	8,468.00	3.037	38.63%	2,740.00	7.916	5.166	2.893	15.975	0.396	0.494	2.236	3.126
DETAILED_S_1_mod	92.890	14.512	18.52%		1,778.701	149,681.179	-275.722	-0.18%					6.750	59.31%	3,605.73	5.773	2.971	2.231	10.974	0.406	0.360	0.968	1.734
SIMPLIFIED_S_1_H	123.97			151,459.880	2,390.806	149,069.074			37.865	6,025.590	22.012	8,468.00	3.037	38.80%	2,740.00				13.842				0.993
SIMPLIFIED_S_1_mod_H	163.11	39.143	31.57%		3,091.099	148,368.78	-700.294	-0.47%					6.750	59.35%	3,606.00				10.129				0.889
DETAILED_S_1_H	124.737			151,459.880	2,356.687	149,103.193			37.865	6,025.590	22.012	8,468.00	3.037	38.63%	2,740.00	7.916	5.166	2.893	15.975	0.396	0.494	2.236	3.126
DETAILED_S_1_mod_H	164.057	39.320	31.52%		3,070.546	148,389.335	-713.858	-0.48%					6.750	59.31%	3,606.00	5.773	2.971	2.231	10.974	0.406	0.360	0.968	1.734
2040						**2040**																	
SIMPLIFIED_S_2	77.56			159,321.653	1,510.946	157,810.706			39.830	6,629.530	25.393	9,551.00	3.012	37.17%	1,500.00				12.755				1.771
SIMPLIFIED_S_2_mod	89.26	11.694	15.08%		1,576.847	157,744.81	-65.901	-0.04%					5.137	54.42%	1,500.00				9.297				1.505
DETAILED_S_2	78.723			159,321.653	1,463.831	157,857.821			39.830	6,629.53	25.393	9,551.00	3.012	37.00%	1,500.00	7.403	4.879	2.724	15.006	0.708	0.774	0.774	2.257
DETAILED_S_2_mod	90.879	12.156	15.44%		1,547.251	157,774.402	-83.419	-0.05%					5.137	54.37%	1,500.00	5.361	2.788	2.050	10.200	0.689	0.539	1.180	2.408
SIMPLIFIED_S_2_H	122.03			159,321.653	2,341.564	156,980.089			39.830	6,629.530	25.393	9,551.000	3.012	0.372	1,500.00				12.755				1.771
SIMPLIFIED_S_2_mod_H	154.56	32.526	26.65%		2,635.382	156,686.27	-293.818	-0.19%					5.137	0.544	1,500.00				9.297				1.505
DETAILED_S_2_H	123.118			159,321.653	2,293.810	157,027.843			39.830	6,629.53	25.393	9,551.00	3.012	37.00%	1,500.00	7.403	4.879	2.724	15.006	0.708	0.774	0.774	2.257
DETAILED_S_2_mod_H	156.126	33.008	26.81%		2,605.417	156,716.235	-311.608	-0.20%					5.137	54.37%	1,500.00	5.361	2.788	2.050	10.200	0.689	0.539	1.180	2.408
2050_1						**2050_1**																	
SIMPLIFIED_S_3	74.20			167,183.425	1,370.764	165,812.661			41.796	7,233.460	32.662	12,104.000	2.716	30.87%	1,500.00				10.516				4.015
SIMPLIFIED_S_3_mod	83.14	8.941	12.05%		1,394.859	165,788.57	-24.095	-0.01%					4.279	44.52%	1,500.00				7.671				3.097
DETAILED_S_3	76.625			167,183.425	1,318.812	165,864.613			41.796	7,233.46	32.662	12,104.00	2.716	30.75%	1,500.00	6.150	4.245	2.323	12.718	1.690	1.418	3.108	6.217
DETAILED_3_mod	86.217	9.592	12.52%		1,360.893	165,822.532	-42.081	-0.03%					4.279	44.49%	1,500.00	4.448	2.416	1.703	8.567	1.510	0.915	1.568	3.993
SIMPLIFIED_S_3_H	111.21			167,183.425	2,086.853	165,096.572			41.796	7,233.460	32.662	12,104.000	2.716	30.87%	1,500.00				10.516				4.015
SIMPLIFIED_S_3_mod_H	136.58	25.371	22.81%		2,269.949	164,913.48	-183.096	-0.11%					4.279	44.52%	1,500.00				7.671				3.097
DETAILED_S_3_H	113.520			167,183.425	2,034.079	165,149.346			41.796	7,233.46	32.662	12,104.00	2.716	30.87%	1,500.00	6.150	4.245	2.323	12.718	1.690	1.418	3.108	6.217
DETAILED_S_3_mod_H	139.609	26.089	22.98%		2,235.875	164,947.550	-201.796	-0.12%					4.279	44.52%	1,500.00	4.448	2.416	1.703	8.567	1.510	0.915	1.568	3.993
2050_2						**2050_2**																	
SIMPLIFIED_S_4	65.04			167,183.425	1,021.362	166,162.064			41.796	7,233.460	47.702	17,336.000	1.649	19.30%	1,500.00				6.980				8.397
SIMPLIFIED_S_4_mod	71.48	6.445	9.91%		1,052.753	166,130.67	-31.392	-0.02%					2.718	28.93%	1,500.00				5.161				5.967
DETAILED_S_4	70.178			167,183.425	946.601	166,236.824			41.796	7,233.46	47.702	17,336.00	1.649	19.23%	1,500.00	4.323	3.091	1.477	8.891	3.561	2.602	4.148	10.311
DETAILED_S_4_mod	77.637	7.459	10.63%		992.069	166,191.356	-45.469	-0.03%					2.718	28.93%	1,500.00	3.088	1.723	1.118	5.929	2.897	1.626	2.215	6.737
SIMPLIFIED_S_4_H	88.22			167,183.425	1,463.142	165,720.283			41.796	7,233.460	47.702	17,336.000	1.649	19.30%	1,500.00				6.980				8.397
SIMPLIFIED_S_4_mod_H	106.19	17.977	20.38%		1,613.964	165,569.46	-150.822	-0.09%					2.718	28.93%	1,500.00				5.161				5.967
DETAILED_S_4_H	93.255			167,183.425	1,386.519	165,796.906			41.796	7,233.46	47.702	17,336.00	1.649	19.23%	1,500.00	4.323	3.091	1.477	8.891	3.561	2.602	4.148	10.311
DETAILED_S_4_mod_H	112.349	19.094	20.48%		1,548.170	165,635.255	-161.650	-0.10%					2.718	28.93%	1,500.00	3.088	1.723	1.118	5.929	2.897	1.626	2.215	6.737

Dmitrijs Guzs was born in 1985 in Jelgava, Latvia. He received a Master's degree in Energy Physics from the Norwegian University of Life Sciences in 2009 and a Master's degree in Electrical Power Engineering from RWTH Aachen in 2014. He has been employed at "Statkraft Energi AS", "Bayer Technology Services GmbH", and "AS Augstsprieguma Tīkls". Since 2022, he has been a senior engineer in the Baltic RCC. His scientific interests are power system frequency stability, load shedding schemes and power system socioeconomic welfare calculations.